

# Decentralized Advanced Model Predictive Controller of Fluidized-Bed for Polymerization Process

**Ahmed S. Ibrahem\***<sup>+</sup>

*Department of Chemical Engineering, UiTM University of Mara 40450 Shah Alam, MALAYSIA*

**Mohamed A. Hussain**

*Department of Chemical Engineering, University of Malaya 50603 Kuala Lumpur, MALAYSIA*

**Nayef M. Ghasem**

*Department of Chemical Engineering, University of Al Ain. U.A.E*

**ABSTRACT:** *The control of fluidized-bed operations processes is still one of the major areas of research due to the complexity of the process and the inherent nonlinearity and varying dynamics involved in its operation. There are varieties of problems in chemical engineering that can be formulated as NonLinear Programming (NLPs). The quality of the developed solution significantly affects the performance of such system. Controller design involves tuning the process controllers and implementing them to achieve certain performance of controlled variables by using Sequential Quadratic Programming (SQP) method to tackle the constrained high NLPs problem for modified mathematical model for gas phase olefin polymerization in fluidized-bed catalytic reactor. The objective of this work is to present a comparative study; PID control is compared to an advanced neural network based MPC decentralized controller and also, see the effect of SQP on the performance of controlled variables. The two control approaches were evaluated for set point tracking and load rejection properties giving acceptable results.*

**KEY WORDS:** *Model predictive control, Proportion integral derivative control, Neural networks, Optimization.*

## INTRODUCTION

The incentive for process control may vary depending on the processes application under consideration. The objectives include; maintaining high product quality, avoiding or minimizing losses, maximizing throughput, minimizing operational costs, and ensuring safe and an environment friendly operation. Furthermore, studying the control of fluidized-bed, polymerizations operations

has always been a research active area because of its complexity and non-linearity that obscure the design of optimum control strategies capable of handling the whole ranges of operation. This is further complicated by the availability of a variety of contacting geometries, and the use of diverse processing techniques. The processes entailed in fluidization are highly complex and often

---

\* To whom correspondence should be addressed.

+ E-mail: [ahmed\\_ibrahem@salam.uitm.edu.my](mailto:ahmed_ibrahem@salam.uitm.edu.my)

1021-9986/12/4/91

27/\$/4.70

require extensive coordination and management in order to ensure that they are handled efficiently and with high safety standards. The ability of the process to achieve and maintain the desired equilibrium value is termed as the controllability of the process. This is measured by considering a range of properties of the non linear process [1]. However, in engineering practice a plant is called controllable if it is possible to achieve the specified control objectives [47]. Control strategy involves the design of control systems and studying them for stability and robustness. Controller design involves tuning the process controllers and implementing them to achieve certain performance of controlled variables. Nevertheless, most industrial polymerization processes are still controlled using linear controllers based on linear process model. However starting from the last decade, some researchers [31],[5],[13] have started proposing nonlinear controller designs to control certain severely nonlinear processes where tight control is required. Furthermore, most of the nonlinear control problems related to polyethylene reactors are highly complex. This process is represented one of the major challenges facing process engineers in the chemical process industries and this process requires optimization and control of product quality while keeping process variable costs as low as possible.

Modern control algorithms attempt to address these difficulties and to solve the polymerization control problem under variable operating conditions in order to achieve optimal performance. Many such algorithms have been proposed during the last two decades [2].

Recently, the Model Predictive Control (MPC) has attracted researchers as well as process engineers to implement it as one of the most recommended advance process algorithms, both in academic and industry. The combination of new control design concepts in MPC, such as model prediction, receding horizon optimization and real time correction, makes it possible to yield high performance characteristics and Neural Network (NN) based control system design is gaining a great deal of attention due to the networks universal approximation ability, on and off learning feature, and their parallelism [4],[6].

Control studied for the polyethylene production process spans a variety of schemes and algorithms. A list of relevant studies is given in Table 1 for the period 1990-2008 [8].

In this work, we have utilized the advantages of both methods within a neural-network model based model

prediction controller to control the fluidized bed polyethylene reactor. The model used for the control is the modified model developed recently by [1]. Control studies were done for set point tracking and disturbance rejection and comparison made with the PID controller.

## THEORETICAL SECTION

### *Descriptive behavior of the new mathematical model*

Heterogeneous models are used widely especially in polymerization system. Current research in this important area can be divided into two parts namely; mathematical models for fixed bed catalyst reactor systems and mathematical models for fluidized bed catalytic reaction for production of polyethylene [29],[71],[23] improved the heterogeneous model however, they did not consider solid phase effect. *Varma*, 1981 included mixing in the axial direction. *R. Sala, F. Valz-Gris & L. Zanderighi* Paterson developed a two dimensional mathematical model where concentration and temperature patterns in the reactor can be predicted [11],[12]. *R.J. Zeman & N. R. Amundson, Xuejing Zheng, Makarand S. Pimplapure, Günter Weickert, and Joachim Loos, Victor M. Zavala, Antonio Flores-Tlacuahuac and Eduardo Vivaldo-Lima* improved the Dynamic optimization of a semi-batch reactor for polyurethane production, *H. Hatzantonis, H. Yiannoulakis, A. Yiagopoulos, C. Kiparissides* further improved the two phase model of the polymerization system. In previous works, mass transfer with chemical reaction in fluidized-bed systems either consider all phases (*D. Kunii & O. Levenspiel*, 1969) or the emulsion phase alone [31],[5],[13].

Modified modeling is by including the catalyst phase and considering all three phases as compared to the other models i.e, constant bubble size model, well mixed model and the bubble growth model. Simulations were also performed to study the effect of superficial velocity and catalyst flow rate in the bubble and emulsion phases. Comparisons with actual plant data at steady state were also performed [1],[17].

In this model the reactant gas enters the bottom of the bed and flows up the reactor in the form of bubbles. As the bubbles rise, mass transfer of the reactant gases takes place between the bubbles and the clouds without chemical reaction, and between the clouds and the emulsion without chemical reaction, and between emulsion and solid with a chemical reaction that happened

Table 1: Summary of control studies for polymerization processes from 1990 to 2008.

No	Researcher	Year	Control system	Control strategy	Product
1	Elnashaie, Gonzales Velasco, Abdel-Hakim	1990	Deadbeat method	Set point (Temperature) effect of batch reactor	Polyethylene
2	G. Ravi, Y. Arkun, F. Joseph	1994	NLMPC	Set point (Temperature and Concentration) effect of batch reactor	Polyethylene
4	Wei, Danial	1996	IMC	Control relevant reduction of volterra series models	Polymerization process
6	Thomas, Francis	1997	IMC	An anti-windup scheme for multivariable nonlinear systems	Polymerization process
7	Tian,y.J.Zhang, A.J.Morris	1999	Neural network	Set point (Temperature) effect of batch reactor	Polyethylene
8	A.Bolsoni,E.L.Lima, J.C.Pinto	1999	Predictive control	Set point (Concentration) effect of batch reactor	Polystyrene
9	Morimasa, Masahiro, Koji, Fuminao	1999	Predictive control	Control melt index	Polyethylene
10	Gangadhar, Evangelhos	1999	Optimal controller	Set point (Temperature) effect of batch reactor	Polystyrene
11	Janos, Lagos, Ferenc	2000	Fuzzy control	Set point (Temperature) effect for batch reactor	Polystyrene
12	Yaohui, Yaman	2000	Predictive control	Set point (Concentration) effect of batch reactor	Emulsion Polymerization system of polystyrene
13	Janson, Lajos, Ferenc	2000	Fuzzy	Distributed (Temperature) effect for batch reactor	Emulsion Polymerization system
14	Boong, Goon, Kee, Hyun	2001	Predictive control	Distributed (Temperature) effect for batch reactor	Methyl Methacrylate
15	W.C.Chen, Ni-Bin. Chang, Jenj	2001	Fuzzy neural control	Distributed (Temperature) effect for batch reactor	polypropylene
16	Boong, Kee, Hyu	2001	MPC	Set point (Temperature and Concentration) effect of batch reactor	Polystyrene
17	O. Abel, W. Marquardt	2001	Predictive control	Set point (Temperature and Concentration) effect of batch reactor	Polystyrene
18	Joachim Horn	2001	Neural network	Set point (Temperature and Concentration) effect of batch reactor	Polypropylene
19	Hiroya, Morimasa, Satoshi, Kouji, Masahiro, Wang	2001	Predictive control	Set point Temperature effect of batch reactor	Polyethylene
20	Robert, Douglas, Ronald, Babatund	2001	Volterra series model	Identification of nonlinear empirical models for chemical dynamic processes	Polystyrene
21	C.W.Ng, M.A.Hussain	2002	Hybrid neural network	Distributed (Temperature) effect for batch reactor	Polymerization process
22	Charles, Francis	2002	Open loop optimal	Control of particle size distributaries	Emulsion Polymerization system
23	Yuan, Jie, Julian	2002	Optimal control	Control of particle size distributaries and composition	Emulsion Polymerization system
24	Dulce, Nuno	2002	MPC	Control of particle size distributaries and composition of batch polymerization system	Vinyl chloride and methyl methacrylate
25	Sang, Hyun	2002	Auto-regressive moving average model	Set point (Temperature and Concentration) effect of continuous system	Polystyrene

Table 1: Continued

26	Chiaki, Jinyoung	2002	Neural network	Set point (Temperature effect of batch reactor system	Emulsion Polymerization system
27	Nayef Mohamed Ghasem	2005	Optimal control	Distributed (Temperature) effect for batch reactor	Emulsion Polymerization system
28	Zhihua, Jie	2004	Optimal control	Batch-to –Batch control	Poly Methyl methacrylate
29	Nido, Gilles, Timothy	2003	MPC	Set point (Concentration) effect of batch reactor linear system	Polystyrene
30	Kenneth, Ahmet	2003	IMC	Control for nonlinear process change in set point concentration	Polystyrene
31	Francis, Christopher, Timothy	2003	MPC	Control of particle size distribution in batch reactor	Emulsion Polymerization
32	R.A.M. Vieira, M. Embirucu, C. Sayer, Lima	2003	MPC	Control of particle size distribution in batch reactor set point concentration	Polystyrene
33	C.Chatziduksa, J. D Perkins, C. Kiparissides	2003	Optimal control	Set point (Concentration) effect of fluidized bed reactor	Polyethylene
34	D. Del Vecchio, N. Petit	2005	Optimal control	Control for tubular chemical reactor	Polystyrene
35	Antonio, Lorenz	2005	Optimal control	Control for unstable polymerization reactors	Polystyrene
36	G. Mourue, D. Dochain, V.Wertz, D. Descamps	2004	MPC	Distributed concentration effect for nonlinear chemical processes	Polystyrene
37	Z. Zeybek, S. Yuce, H.Hapoglu, M. Alpaz	2004	Adaptive controller	Control heuristic temperature of batch reactor	Polystyrene
38	Dennis, Okko	2005	Predictive control	Distributed (Temperature and concentration) effect for continuous nonlinear chemical processes	Polyethylene
39	Costas Kiparissides	2005	Optimal control	Control on molecular weight distribution	Polyethylene
40	Simant, Baranitharan, Ali	2005	Optimal control	Control for determination of MMA polymerized in non-isothermal batch reactor	Poly Methyl methacrylate
41	Ch. Vekates, K. Venkat	2005	Neural network	Control of unstable nonlinear processes	Poly Methyl methacrylate
42	Jesus, Cerrillo, John	2005	MPC	Distributed (Temperature and Pressure) effect for autoclave process	Nylon polymerization autoclave process
43	Babatunde, Ogunnaike, Kapil	2006	MPC	Control of nonlinear processes	Polystyrene
44	Bassam, Jose	2006	Optimal control	Control on emulsion copolymerization of styrene	Poly Styrene
45	B.Alhamad, R. Willis, J. A. Romagnoli, Gomes	2006	Optimal control	Control on molecular weight distribution	Poly Styrene
46	Felix, Masound, Michael	2006	Optimal control	Control of high temperature semi batch reactor	Poly butyl acrylate
47	Ahmmed s ibrehem, Mohamed Azlan Hussain, Nayef Mohamed Ghasem	2007	NMPC	Control of emulsion temperature and molecular weight	Poly ethylene
48	Sebastian Terrazas-Moreno, Antonio Flores-Tlacuahuac, and Ignacio E. Grossmann	2008	Optimal control	Control of temperature	Poly Methyl methacrylate

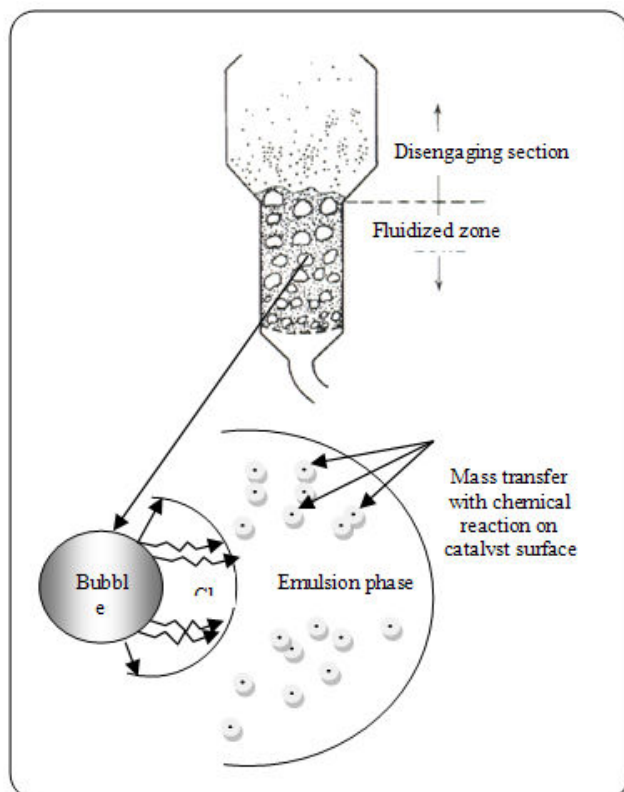


Fig. 1: Steps of polymerization process.

on the surface of catalyst particles, and specify the kind of catalyst particles if the catalyst porous or rigid kind because the kind of catalyst particles has big effects on the rate of reaction. All details can be shown in [1],[17].

In this model the reactant gas enters the bottom of the bed and flows up the reactor in the form of bubbles. As the bubbles rise, mass transfer of the reactant gases takes place between the bubbles and the clouds without chemical reaction, and between the clouds and the emulsion without chemical reaction, and between emulsion and solid with a chemical reaction that happens on the surface of catalyst particles. The model accounts the effects of solid phase on the rate of reaction as shown in Fig. 1.

The product then flows back into the bubble and finally exits the bed when the bubble reaches the top of the bed. The rate at which the reactants and products transfer in and out of the bubble affects the conversion but the time delay of bubble is very small.

The bubbles contain very small amounts of solids. They are not spherical; rather, they have an approximately hemispherical top and a pushed-in bottom.

Each bubble of gas has a wake which contains a significant amount of solids [35],[54],[55].

As the bubble rises, it pulls up the wake with its solids behind it. The net flow of the solids in the emulsion phase must therefore be downward. The gas within a particular bubble remains largely within that bubble, penetrating only a short distance into the surrounding emulsion phase. The region penetrated by gas from a rising bubble is called the cloud. Emulsions are part of a more general class of two-phase systems of matter called colloids. Although the terms colloid and emulsion are sometimes used interchangeably, emulsion tends to imply that both the dispersed and the continuous phase are liquid. The model assumptions are listed in Table 2 and the difference in assumptions between our model and the entire well known model is shown in Table 3 [37], [39], [56].

#### Reaction kinetics

(A). the specific properties of this step for rigid catalyst particles are as, follow;

After the mass transfer of emulsion particles to the catalyst, chemical reaction will happen on the surface of catalyst if the catalysts are not porous.

The polymerization rate in the gas phase obtained with the type of catalyst used in this work clearly shows growing polymer chain by depending on active site that happen at the surface layers of catalyst. Many models are not concerned about what happen exactly between emulsions molecules and catalysts particles so, in this proposed model we try to give a good picture about what happen at these catalysts particles by depending on the kind of the rate of reaction at the surface of catalyst particles as seen in Fig. 2 so, as to calculate propagation growth of polyethylene particles [58], [62].

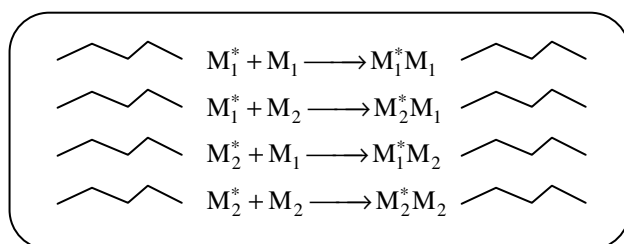
The rate of reaction in catalyst is surface reaction of reactants compounds to form products compounds. From above it is important to use fluidized-bed heterogeneous catalyst in polymerization process so, as to specify the mathematical model formation. Regardless of the specific geometry used to contact the gas and the solid, all these schemes require a complex set of mass, heat transfer and reaction steps and all these steps can influence the overall reaction and mathematical model design for polymerization process [40], [63].

**Table 2: List of model assumptions.**

1- The fluidized bed comprises of three phases: bubble, cloud, emulsion and solid phases.
2- Polymerization reactions occur in emulsion and solid phases.
3- The emulsion phase is at minimum fluidizing conditions.
4- Gas in excess of that required to maintain the minimum fluidizing condition passes through the bed as the bubble phase.
5- There are negligible radial temperature and concentration gradients in the bed, due to the agitation produced by the up-flowing gas.
6- There is not negligible resistance to mass transfer between emulsion and solid phase.
7- The gas phase is composed of ethylene, 1-butene, nitrogen and hydrogen.
8- The dynamic of reactions is represented by the rate of reaction at the surface of two kinds of catalysts i.e., rigid and porous catalysts.
9- In this model mass transfer of emulsion molecules occurs on the catalyst solid particles and react at the surface of catalysts particles (surface reaction) with propagation of polymer particles.

**Table 3: Shows the differences between the mathematical model and the other models.**

No	Functions	Mathematical model	Constant bubble size model	Bubble growth model	Well-mixed model
1	Phases	Bubble cloud emulsion solid phase	Bubble Emulsion	Bubble Emulsion	One Phase
2	Mass transfer from bubble to the cloud	calculated without chemical reaction	Not calculated	Not calculated	Not calculated
3	Mass transfer from cloud to the emulsion	calculated without chemical reaction	Mass transfer from bubble to the emulsion with chemical reaction	Mass transfer from bubble to the emulsion with chemical reaction	One temperature and concentration change represented by one phase only
4	Mass transfer from emulsion to the solid	Mass transfer from emulsion to the solid with a chemical reaction	Not found	Not found	Not found
5	Rate of reaction	Two types of rate of reaction for catalysts porous and rigid.	Activation reaction not depending on the types of catalysts	Activation reaction not depending on the types of catalysts	Activation reaction not depending on the types of catalysts
6	Energy transfer	Solid phase considered	Solid phase ignored	Solid phase ignored	Solid phase ignored

**Fig. 2: Four plausible polymerization steps**

In the simplest case, where only two monomers  $M_1$ ,  $M_2$  are involved, the four plausible polymerization steps can be illustrated in Fig. 2 as follows.

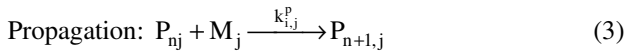
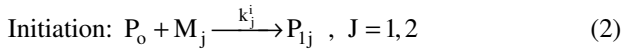
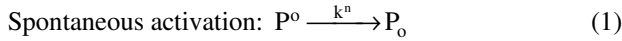
The kinetic mechanism of ethylene-butene copolymerization involves a large number of simultaneous and parallel reactions and a myriad of inorganic species. The kinetic mechanism of copolymerization can be found

in de *Carvalho et al.*, *McAuley et al.*, and *Xie et al.*, which are adapted from the earlier kinetic models of *Bohn & Kissin* [41],[45].

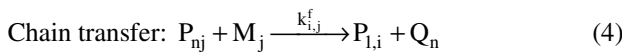
In these kinetic models, only the effects of the terminal monomer on reaction rates are considered, the effects of chain-length and penultimate effects are neglected. Generally, the chemical species considered in this modified mathematical model are active sites, cocatalyst, live polymers, dead polymers, chain transfer agent, impurities, and poison.

The concentration of these species is denoted by a pair of bracket enclosing the species, the concentration of ethylene, butane, hydrogen, potential active sites, active sites, live polymers, and dead polymers are represented by  $[M_1]$ ,  $[M_2]$ ,  $[H_2]$ ,  $[P^0]$ ,  $[P_{n,i}]$  and  $[Q_n]$  respectively [71],[33],[46],[69].

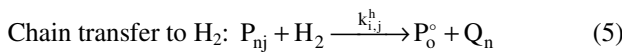
When supported catalyst particles are injected into the polymerization reactor, the chemical species take part in a series of complex reactions at the interface between the solid catalyst and the polymer matrix, as follows.



$$i, j = 1, 2, \quad n = 1, 2, \dots, \infty$$



$$i, j = 1, \quad n = 1, 2, \dots, \infty$$



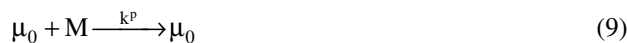
$$i, j = 1, 2, \quad n = 1, 2, \dots, \infty$$

The reaction begins by the formation of active sites (1), which is assumed to take place in excess of cocatalyst. This reaction is followed by initiation reactions (2), in which the monomer gases and the active sites are combined to form live polymers. The live polymers then grow according to the propagation reactions (3). Most dead polymers are produced by chain transfers reactions, which can occur in several ways [48], [49]. For simplicity, only chain transfers to monomers (4) and hydrogen (5) are considered in the kinetic modeling. From the kinetic mechanism, the rate expression for each species can be written and the rate expression for the active sites  $r_{p0}$  can be written as follows:

$$r_{p0} = \text{Active site formation} - \text{Active site consumption}$$

$$k^n [P^0] - \sum_{j=1}^2 k_j^i [P_0] [M_j] \quad (6)$$

It is therefore desirable if the kinetics and rate expressions could be manipulated to a simple form. So, the kinetic mechanism outlined in Eq. (1-5) may be viewed as if it is equivalent to the pseudo kinetic mechanism below:



When  $[M], \mu_0, v_0$  are the collective representations of the concentrations of the monomers, live polymer, and the dead polymer. Table 4 gives the simplified form of terms that are found the rate expressions of the species, using method of pseudo kinetic rate constants [64],[65].

For binary copolymerization system, *H. Tobita & A. E. Hamielec*, 1991, have shown that

$$\phi_1 = \frac{k_{2,1}^p f_1}{k_{2,1}^p f_1 + k_{1,2}^p f_2} \quad (12)$$

$$\phi_2 = \frac{k_{1,2}^p f_1}{k_{2,1}^p f_1 + k_{1,2}^p f_2} \quad (13)$$

Therefore the pseudo kinetic constants can be written as follows:

$$k^i = \sum_{j=1}^2 k_j^i [M_j] / \sum_{j=1}^2 [M_j] \quad (14)$$

$$k^h = \sum_{i=1}^2 k_i^h k_{2-[i/2],i}^p [M_i] / \sum_{i=1}^2 k_{2-[i/2],i}^p [M_i] \quad (15)$$

$$k_j^h = \sum_{i=1}^2 k_{i,j}^h k_{2-[i/2],i}^p [M_i] / \sum_{i=1}^2 k_{2-[i/2],i}^p [M_i] \quad (16)$$

$$k_j^p = \sum_{i=1}^2 k_{i,j}^p k_{2-[i/2],i}^p [M_i] / \sum_{i=1}^2 k_{2-[i/2],i}^p [M_i] \quad (17)$$

$$k^p = \sum_{j=1}^2 k_j^p [M_j] / \sum_{j=1}^2 [M_j] \quad (18)$$

$$k^f = \sum_{j=1}^2 k_j^f [M_j] / \sum_{j=1}^2 [M_j] \quad (19)$$

The dynamic mass balance for the catalyst is as follows:

Accumulation = in by flow - out by flow

$$\frac{dC_{cat}}{dt} = \frac{F_{cat}}{W_s} - \frac{Q_0 C_{cat} P_{cat}}{W_s} \quad (20)$$

Similarly, the mass balance for the potential active sites and active sites, which are

Table 4: Simplified terms in rate expression.

Term in rate expressions	Simplified form
$\sum_{j=1}^2 [M_j]$	[M]
$\sum_{n=1}^{\infty} \sum_{j=1}^2 [P_{n,i}]$	$\mu_0$
$\sum_{n=1}^{\infty} [Q_n]$	$v_0$
$\sum_{n=1}^{\infty} \sum_{i=1}^2 \sum_{j=1}^2 k_{i,j}^p [P_{n,i}] [M_j]$	$\sum_{i=1}^2 \sum_{j=1}^2 k_{i,j}^p [\phi_i \mu_0] [f_j M]$
$\sum_{i=1}^2 \sum_{j=1}^2 k_{i,j}^p [\phi_i \mu_0] [f_j M]$	$k^p \mu_0 [M]$
$\sum_{n=1}^{\infty} [P_{n,i}] / \sum_{n=1}^{\infty} \sum_{i=1}^2 [P_{n,i}]$	$\phi_i$
$[M_j] / \sum_{j=1}^2 [M_j]$	$f_i$
$\sum_{j=1}^2 k_j^i [M_j]$	$k^i [M]$
$\sum_{n=1}^{\infty} \sum_{i=1}^2 k_{i,j}^h [P_{n,i}]$	$k^h \mu_0$
$\sum_{n=1}^{\infty} \sum_{i=1}^2 k_{i,j}^p [P_{n,i}]$	$k^p \mu_0$
$\sum_{n=1}^{\infty} \sum_{i=1}^2 \sum_{j=1}^2 k_{i,j}^p [P_{n,i}] [M_j]$	$k^p \mu_0 [M]$
$\sum_{n=1}^{\infty} \sum_{i=1}^2 \sum_{j=1}^2 k_{i,j}^f [P_{n,i}] [M_j]$	$k^f \mu_0 [M]$

$$\frac{d[P^0]}{dt} = \frac{F_{cat} P_{in}^0}{W_S} - \frac{Q_0 P^0 \rho_{cat}}{W_S} - r_{P^0} \quad (21)$$

$$\frac{d[P_0]}{dt} = \frac{F_{cat} P_0}{W_S} - \frac{Q_0 P_0 \rho_{cat}}{W_S} - r_{P_0} \quad (22)$$

The dynamic molar balances for all other species  $X^k$ , (e.g.,  $\mu_0^k, \mu_1^k, \mu_2^k, v_0^k, v_1^k, v_2^k$ ) can be expressed as

$$\frac{dX^k}{dt} = R_X^k - \frac{Q_0 X^k \rho_{cat}}{W_S} \quad (23)$$

These leading moments are used in the calculation of weight average molecular weight  $M_w$  and number average molecular weight  $M_n$ .

$$W = \sum_{j=1}^2 W_j [M_j] / \sum_{j=1}^2 [M_j] \quad (24)$$

$$M_n = W \left( \frac{\mu_1 + v_1}{\mu_0 + v_0} \right) \quad (25)$$

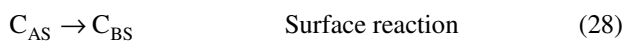
$$M_w = W \left( \frac{\mu_2 + v_2}{\mu_1 + v_1} \right) \quad (26)$$

Where  $W_j$  is the molecular weight of the monomer / comonomer.

(B). the specific properties of this step for porous catalyst particles are as, follows;

In this study the polymerization with less porous catalyst particles tends to take place first only at the exit of a particle due to the emulsion molecules diffusion and chemical reaction happening at the exit surface of catalyst particle then emulsion particles can easily diffuse into the porous of the catalyst particles[50],[51],[59].

The reactant adsorption as represented by Eq. (27), the surface reaction as represented by Eq. (28), and the product desorption as represented by Eq. (29) to produce the overall reaction of equation represented by Eq. (30) as, seen below;



Rate of surface reaction is the controlled reaction, where the rate of adsorption and the rate of desorption is limited as, seen below: Eqs. (31) and (33) will be reduced to the following:

Rate of reaction adsorption

$$r_{AD} = K_A (P_A C_V - C_{AS} / K_A) \quad (31)$$

Rate of reaction in the surface:

$$r_S = K_S (C_{AS} - C_{BS} / K_S) \quad (32)$$

Rate of desorption:

$$r_D = K_D (C_{BS} - C_B / K_D) \quad (33)$$

The overall reaction must be controlled by the rate of reaction surface so, the rate of adsorption and desorption must be equal zero so as to simplify the solution. Hence,

$$r_{AD} = 0 = K_A (P_A C_V - C_{AS} / K_A) \quad (34)$$

$$P_A C_V = C_{AS} / K_A$$

$$C_{AS} = P_A C_V K_A \quad (35)$$

$$r_D = 0 = K_D (C_{BS} - C_B / K_D) \quad (36)$$

$$C_{BS} = C_B / K_D \quad (37)$$

$$C_T = C_V + C_{AS} + C_{BS} \quad (38)$$

$$C_T = C_V (1 + P_A K_A) + C_B / K_D \quad (39)$$

$$C_A = P_A C_V$$

$$C_A = P_A (C_T - C_B / K_D) / (1 + P_A K_A)$$

From the kinetic mechanism, the rate expression for each species can be written and the rate expression for the active sites  $r_{p_0}$  can be written as follows;

$$r_{p_0} = \text{Active site formation} - \text{Active site consumption} \quad (40)$$

$$= K^n [P^0] - \sum_1^2 K_i^+ C_A$$

$$= K^n [P^0] - \sum_1^2 K_i^+ P_A (C_T - C_B / K_D) / (1 + P_A K_A)$$

So, the pseudo kinetic constants and rate of reactions will be change according to the kind of catalyst as in Eq. (40) so these effects will affect on the live and dead moment's equations in calculation of temperature, concentration of emulsion phase and molecular weight.

The estimation of the reactor model parameters are given in [1]. From Fig.1, it can be seen that the polymerization process in the fluidized bed reactor occurs in three basic steps as, follows:

1. Bubble phase to cloud phase (Step 1).
2. Cloud phase to emulsion phase (Step 2).
3. Mass transfer with chemical reaction from emulsion phase to the catalyst phase and propagation in size and molecular weight of the polyethylene particle (Step 3).

The mass and energy balance equations pertinent to each of these steps are described below where the meaning of all symbols can be found in the nomenclature section.

These steps are giving us a clear picture about operation of polymerization system as see in Fig.1. Many researchers are ignored the relationship between bubble phase and cloud phase; and between emulsion phase and solid phase. The solid phase factor is very important and has big effects on polymerization process because when increased the mass fraction of the catalyst phase in a very small amounts will find a big change will happen in the results of emulsion temperature and concentration [57],[58].

So, in this study will explain in details the three steps with derivative modified mathematical model and all the calculations.

#### Bubble Phase to Cloud Phase of Ethylene (Step 1)

This step represents the first operation step in fluidized bed. Mass transfer from bubble phase to the cloud phase without chemical reaction happens in this step and this assumption is not the same like *Choi & Ray*, *McAuley et al.* and *Hatzantonis* assumptions but this

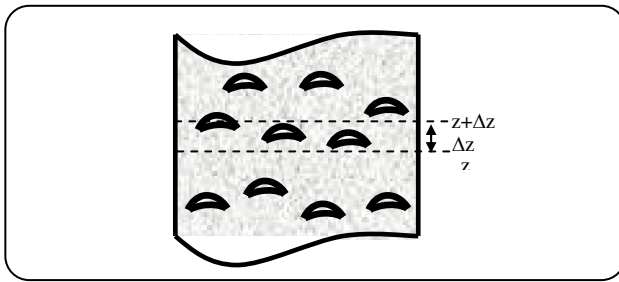


Fig. 3: Section of a bubbling fluidized bed.

assumption different from *D. Kunii & O. Levenspiel* assumption because no chemical reaction that was happened in this step[52],[53].

Material balances will be written over an incremental height  $\Delta z$  for substance A in each of the three phases (bubble, cloud, and emulsion) as seen in Fig. 3.

Mass balance on the bubble phase

The amount of A entering at  $z$  is the bubble phase by flow,

$$(u_b A_c C_{Ab}) \delta = [\text{molar flowrate enter the filled with bubble}] \times [\text{fraction of bed occupied by bubble}]$$

A similar expression can be written for the amount of A leaving in the bubble phase in flow at  $z + \Delta z$ :

In by flow = out by flow + out by mass transport

Dividing by  $A_c \Delta z \delta$  and taking the limit as  $\Delta z \rightarrow 0$  yields

$$(u_b A_c C_{AB})(\delta)_x - (u_b A_c C_{AB})(\delta)_{x+\Delta x} - K_{bc}(C_{AB} - C_{AC}) A_c \Delta z \delta = 0$$

A balance on A in the bubble phase for steady-state operation in section  $\Delta z$  is given by

$$u_b \frac{dC_{Ab}}{dz} = -K_{bc}(C_{Ab} - C_{Ac}) \quad (41)$$

At  $Z = 0$ ,  $C_{Ab} = C_{Ab0}$

Superficial velocity has big effect on monomer temperature because it effects on minimum fluidization velocity, bubble velocity, inlet gas volumetric flow rate to the bubble phase and heat transfer coefficient that leads to direct proportional effects on monomer temperature.

*Energy balance on the bubble phase*

For energy system balance in two states in bubble phase will find the variation of bubble temperature with the height of fluidized bed is the same behavior like *Choi &*

*Ray; McAuley et al.* and *Hatzantonis* assumptions [67],[70].

$$\frac{d}{dz} [C_{Ab}(T_b - T_{ref})] = \frac{H_{bc}}{u_b C_{pg}} (T_c - T_b) \quad (42)$$

*Cloud phase to emulsion phase (Step 2)*

This step represents the second operation step in fluidized bed. Mass transfer from cloud phase to the emulsion phase without chemical reaction happens in this step as seen in Fig. 4 and this assumption is not the same like *Choi & Ray; McAuley et al.* and *Hatzantonis* assumptions because these assumptions not have mass transfer from bubble phase to the cloud phase[72],[73].

Mass balance on the cloud phase

In the material balance on the clouds and wakes in section  $\Delta z$ , it is easiest to base all terms on the bubble volume. The material balance for the clouds and wakes is

Accumulation = in by flow - out by flow + in by mass transport - out by mass transport + generation i.e.

$$0 = \left(\frac{u_c}{\Delta z} C_{Ac}\right)_{\downarrow z} - \left(\frac{u_c}{\Delta z} C_{Ac}\right)_{\downarrow z+\Delta z} + K_{bc}(C_{Ab} - C_{Ac}) - K_{ce}(C_{Ac} - C_{Ae}) + 0$$

$u_c$  (cloud velocity) =

$$u_b \times \frac{V_c (\text{volume of cloud}) + V_w (\text{volume of weak})}{V_{bed} (\text{volume of bed})}$$

Using the *Kunii-Levenspiel* model, the fraction of the bed occupied by the bubbles and wakes can be estimated by material balances on the solid particles and the gas flows. The parameter  $\delta$  is the fraction of the total bed occupied by the part of the bubbles that does not include the wake, and  $\alpha$  is the volume of wake per volume of bubble. The bed fraction in the wakes is therefore  $\alpha\delta$ . The bed fraction in the emulsion phase (which includes the clouds) is  $(1 - \delta - \alpha\delta)$ .

$$\frac{V_c}{V_b} = \frac{3(u_{mf} / \epsilon_{mf})}{u_b - (u_{mf} / \epsilon_{mf})}$$

So, the mass transfer equation from cloud to the emulsion is represented by Eq. (43).

$$u_b \delta \left[ \frac{3(u_{mf} / \epsilon_{mf})}{u_b - (u_{mf} / \epsilon_{mf})} + \alpha \right] \frac{dC_{Ac}}{dz} = K_{bc}(C_{Ab} - C_{Ac}) - K_{ce}(C_{Ac} - C_{Ae}) \quad (43)$$

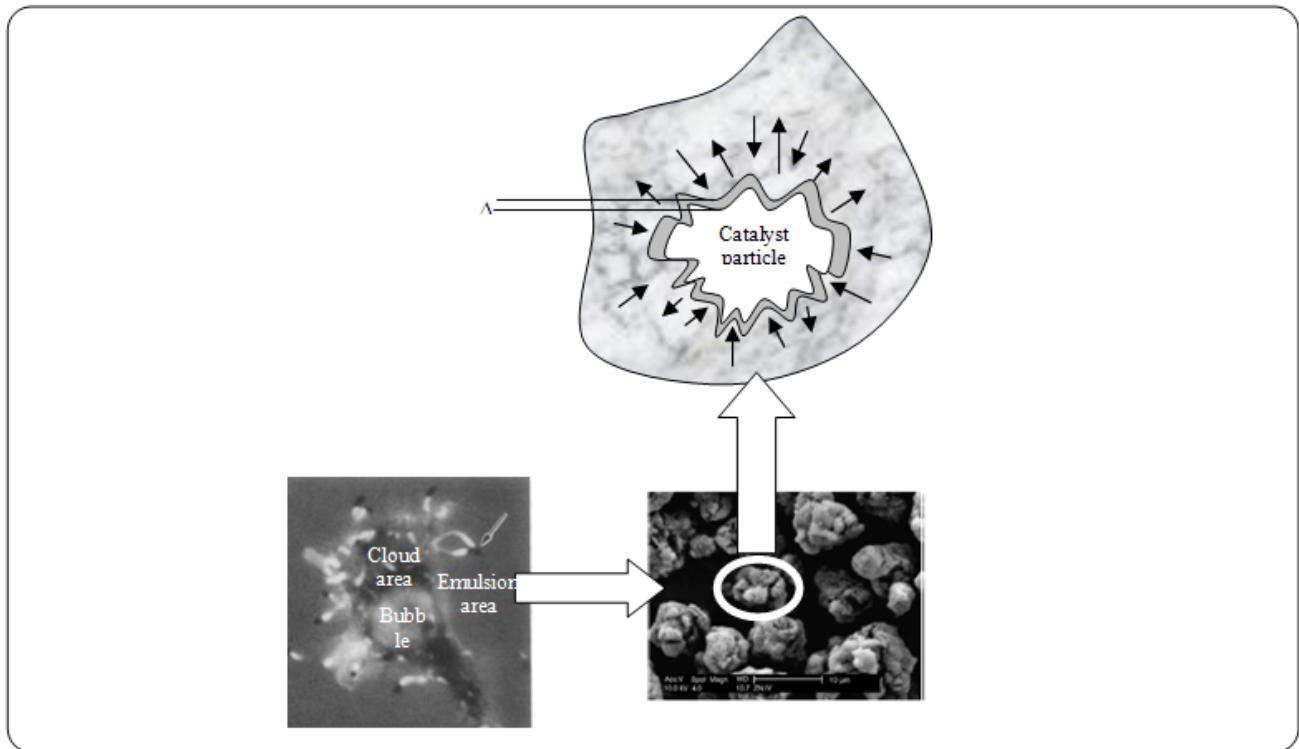


Fig. 4: Shows the mass transfer of emulsion molecules to the catalyst particles Micrography of Ziegler-Natta Catalyst by scanning electron microscope (Wolf et al., 2005).

Energy balance on the cloud phase

For energy balance pass in two states from cloud phase to emulsion phase the variation of cloud temperature with the height of fluidized bed is the same as Choi & Ray; McAuley et al. and Hatzantonis assumptions i.e.

$$\frac{d}{dz} [C_{Ac} (T_c - T_{ref})] = \frac{H_{ce}}{u_c C_{pg}} (T_e - T_c) \quad (44)$$

Mass transfer with chemical reaction from emulsion phase to the catalyst phase and propagation in a size of polyethylene particle (Step 3)

This step represents the third operation step in fluidized bed. Mass transfer from emulsion phase to the catalyst phase with chemical reaction happens in this step as seen in Fig. 4 .and this assumption is not the same like Choi & Ray; McAuley et al. and Hatzantonis.

Mass balance on the emulsion phase

In the material balance on the clouds and wakes in section  $\Delta z$ , it is easiest to base all terms on the bubble volume. The material balance for the clouds and wakes is:

Accumulation = in by flow - out by flow + in by mass transport - out by mass transport + generation i.e.

$$A_1 H \epsilon_{mf} \frac{dC_{Ae}}{dt} = \quad (45)$$

$$K_{ce} [C_{Ac} - C_{Ae}] A_1 H \epsilon_{mf} + \frac{-D_{E,C} A_1 dC_{Ae}}{dr} + r_a W_s$$

To simplify the solution

$$\frac{-D_{E,C} A_1 dC_{Ae}}{dr} = G_1 (C_{AO} - C_{Ae}) - Q_0 C_{Ae} \epsilon_{mf} \quad (46)$$

Where

$D_{E,C}$  Diffusivity of emulsion particles towards catalysts particles ( $m^2/sec$ )

So the Eq. (45) will be:

$$A_1 H \epsilon_{mf} \frac{dC_{Ae}}{dt} = K_{ce} [C_{Ac} - C_{Ae}] A_1 H \epsilon_{mf} + \quad (47)$$

$$G_1 (C_{Ao} - C_{Ae}) - Q_0 C_{Ae} \epsilon_{mf} + r_a W_s$$

Energy balance on the emulsion phase

The energy balance occurs in two states, first from bubble phase to emulsion phase then from emulsion

phase to the solid phase. So, will find the variation of emulsion temperature with the time is not the same behavior as of *Choi & Ray*; *McAuley et al.* and *Hatzantonis* assumptions and is given by.

$$A_1 H \left\{ (1 - \varepsilon_{mf}) \rho_s C_{ps} + \varepsilon_{mf} C_{me} C_{pg} \right\} \frac{dT_e}{dt} + \quad (48)$$

$$A_1 H (T_e - T_{ref}) \varepsilon_{mf} C_{pg} \frac{dC_{me}}{dt} = -GC_{me} C_{pg} (T_e - T_f) +$$

$$A_B H_{be} \int (T_b - T_e) dz + (-\Delta H_r) R_p - Q_0 (\varepsilon_{mf}) C_{me} C_{pg}$$

$$(T_e - T_{fs}) - Q_0 \varepsilon_{mf} C_{me} C_{pg} (T_e - T_f) -$$

$$\pi DH (1 - \delta^*) h_w (T_e - T_w)$$

### Nonlinear model predictive control

Motivated by the advancements of computer technologies and control analysis techniques, more sophisticated control system design procedures have appeared during the past two decades which includes the Nonlinear Model Predictive Controller (NMPC) as mentioned in the previous section.

Model Predictive Control (MPC) refers to a class of algorithms that compute a sequence of manipulated variable adjustments in order to optimise the future behaviour of a plant. Originally developed to meet the specialized control needs of power plants and petroleum refineries, MPC technology can now be found in a wide variety of application areas including chemical production, food processing, automotive, aerospace, metallurgy, pulp and paper industries (*O. Abel et al., 2001*)

The application of MPC for many industrial processes has shown great accomplishments in the past years and it is gaining popularity as an efficient and reliable control algorithm due to its many important features. This feature include its ability to deal with uncertain ties robust to change control objectives, ability to handle process time delays, can handle interacting variables well, in multivariable systems and eliminates stability problems created by constraints[29],[23],[66].

### Neural Network Model Predictive Control technique (NNMPC)

However the strength of the NMPC method depends on the accuracy of the nonlinear model incorporated into the model predictive framework. This is normally difficult in many cases dealing with nonlinear system especially this highly nonlinear polymerization system,

the details of the mathematical model of which can be seen in previous section[3],[7].

However, due to the versatile nature of the Artificial Neural Network (ANN) models for nonlinear systems, it is an excellent candidate to use for modelling the polymerization system and incorporate within the model predictive framework and this is the approach taken to control this system in what is called neural network based model predictive control study[9],[28].

Fig. 5 shows the neural network based MPC scheme. The non-linear optimizer in the MPC is used to select the manipulated variable that minimizes a cost function, which is quadratic in the set point/process output error. To do so, the non-linear optimizer uses the ANN process model to predict the possible future responses of the process to calculate the manipulated variable sequences. By using the ANN model to predict multi-step ahead, the control scheme can anticipate the process trajectory and compensate for measured disturbances before their impact on the process output is detected[14],[47].

The general philosophy of the neural network MPC is identical to that of the standard MPC method. The controller determines a set of future manipulated variable moves that minimize a cost function over a prediction horizon, subject to input and output constraints. The cost function usually includes the sum of squares of the errors between the predicted outputs and the set point values evaluated over the prediction horizon, and commonly also includes a term which penalizes the rate of change of the manipulated variable. For such a cost function, the MPC problem can be posed as follows,

$$\min u(t) J = \sum_{i=P1}^{i=P2} (\tilde{y}(t+i) - r(t+i))^2 + \quad (49)$$

$$\lambda \sum_{i=1}^{i=C} (u(t+i-1) - u(t+i-2))^2$$

where...

$$u(t+i) = u(t+C-1), \quad i \geq C$$

$$u_{\min} \leq u(t) \leq u_{\max}$$

Where J is the cost function to be minimized, P1 to P2 define the prediction horizon, C is the control horizon,  $\tilde{y}(t+i)$  is the predicted process output for time t + i, u(t) is the vector of manipulated variable values of length C and  $\lambda$  is a weighting coefficient. In line with linear MPC,

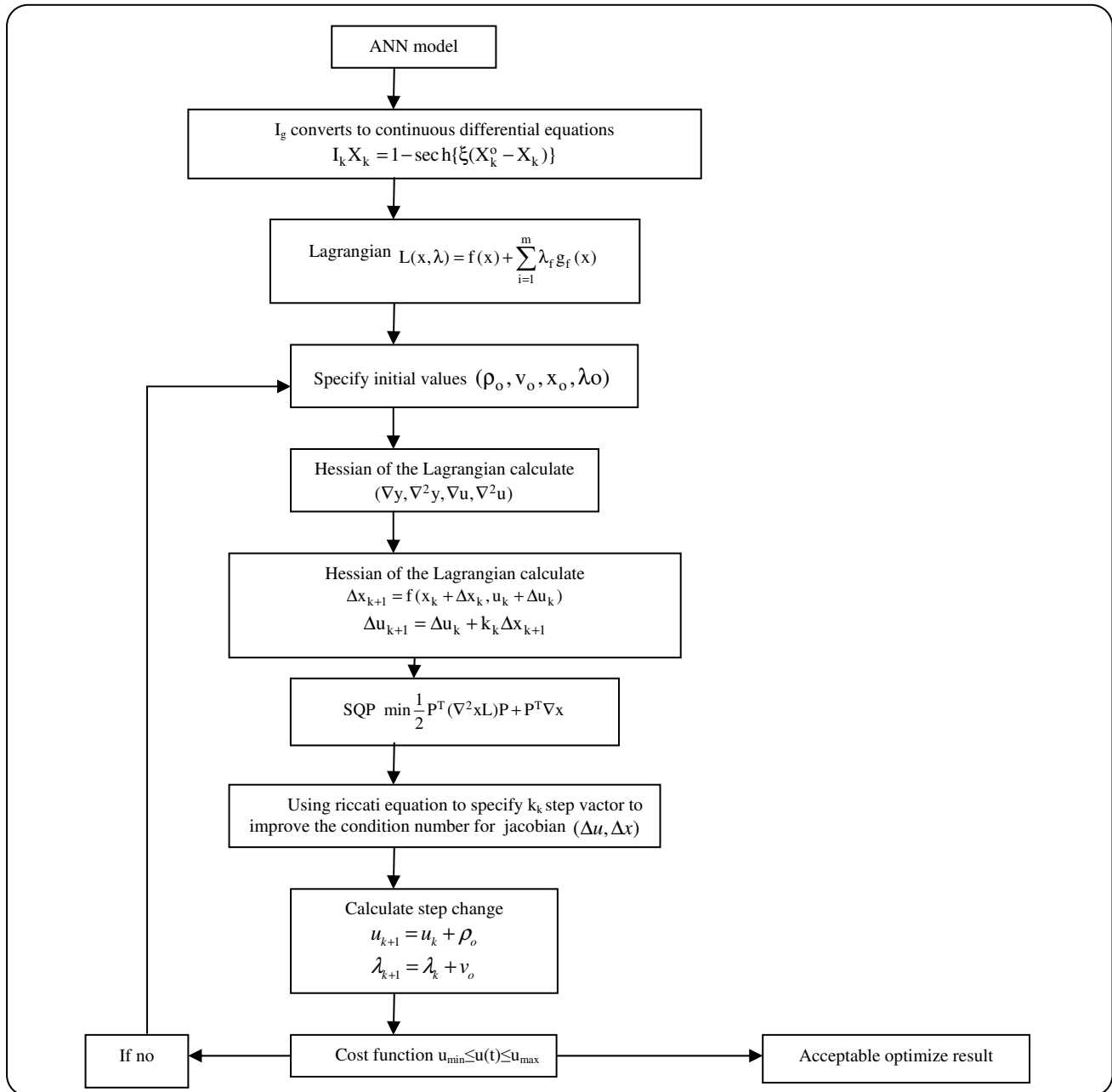


Fig. 5: Represents all optimize control steps.

corrections should be made to the model output to account for process/model mismatch and unmeasured disturbances *Fine T.L. & Smith M.*, and this can be done with an additive disturbance,  $e(t)$  as [14],[47]

$$\tilde{y}(t+i) = \hat{y}(t) + e'(t) \quad (50)$$

Where  $\tilde{y}(t+i)$  is the  $i$ -step ahead ANN model prediction. A simple approach, which was adopted here,

is to use the process/model mismatch to estimate this disturbance, i.e.

$$e'(t) = y(t) - \hat{y}(t) \quad (51)$$

Introduction of the modified set point,  $r'(t)$  gives

$$r'(t+i) = r(t+i) - e'(t) \quad (52)$$

Combining Eqs. (50) to (52) in Eq. (49) gives...

$$\min u(t) J = Q \sum_{i=P1}^{i=P2} (\hat{y}(t+i) - r'(t+i))^2 + \lambda \sum_{i=1}^{i=C} (u(t+i-1) - u(t+i-2))^2 \quad (53)$$

In this study  $y(t)$  represents the emulsion temperature and molecular weight which are the controlled variable and the while variable  $u(t)$  represents superficial velocity and catalyst flow rate. The optimization problem outlined by Eq. (53) is solved using the Sequential Quadratic Programming (SQP) algorithm[155],[21].

#### Sequential Quadratic Programming (SQP)

The SQP method allows us to mimic Newton's method for constrained optimization. At each iteration, a method similar to Newton's method is used to generate a quadratic programming sub problem whose answer is used to determine a search direction for the solution[77].

Since the iterative optimization algorithm employs an analytical gradient method, each term in the control model should be everywhere differentiable. Therefore, the discontinuous binary variable  $I_k$  in the objective function needs to be converted into a continuously differentiable function[20],[79]. In this work,  $I_k$  is approximated by the following smooth function:

$$I_k X_k = 1 - \text{sech}\{\xi(X_k^o - X_k)\} \quad (54)$$

and

$$I_k X_k = 1 - (1/(1/e^{-\xi}(X_k^o - X_k))) \quad (55)$$

Where  $\xi$  is a suitably large number. It tends to rapidly converge from zero to one, as  $(X_k^o - X_k)$  goes from zero to a large value. Therefore, a suitable large  $n$  ensures that it is not only binary but also differentiable. With this approach,  $I_k$  can be converted to a continuously differentiable function at the price of some inaccuracy by approximation. A number of other smooth approximation functions are also available from *Biegler*, 1998 [44],[60],[78].

The computational efficiency associated with solving an optimization problem is often the key concern in the online implementation of MPC methods. However, the conventional MPC methods experience an extremely large computational burden for large-scale manufacturing

processes. The computational burden rapidly increases as the problem size expands. Therefore, to improve the computational efficiency in the on-line optimization, it is necessary to reduce the dimensionality of the optimization problem[16],[61]. For this purpose, we transform the controllable and fixed variables into reduced score variables in the Pulsated prediction model and then optimize for the score variables. A decision variables,  $t_1; \dots; t_A$ , controllable and fixed variables are expressed by

$$X_k = t_1 p_{1,k} + \dots + t_A p_{A,k}, \quad k = 1, \dots, c \quad (56)$$

Where  $p_{A,k}$  is parameters estimation of element  $p_A$  at each  $k$  value.

The objective of optimization is to minimize (or maximize) a function of one or more parameters as in Fig. 5. A set of equality and/or inequality constraints that are also functions of the parameter set, and which confine the parameter values to specified regions of the search space, may also be imposed as part of the optimization problem[22],[75]. A minimization problem may be stated more formally in the following mathematical format: minimize  $F(x)$ , subject to:  $g(x)$  and  $h(x) \geq 0$ ,

where  $x$  is a real-valued vector of variable parameters,  $F(x)$  is a scalar-valued cost function, and  $g(x)$  and  $h(x)$  are vectors of constraint functions. The solution to the general optimization problem is obtained by Lagrange Multiplier analysis[6],[18]. The Lagrangian for the standard optimization problem may be written as

$$L(x, \lambda, \mu) = F(x) - \lambda^T g(x) - \mu^T h(x) \quad (57)$$

Where  $\lambda$  and  $\mu$  are Lagrange multiplier vectors. The following Kuhn-Tucker necessary (*Baker et al*, 2002 and *Fine*, 1999) conditions for a local minimum may be applied to gain potential solutions to this problem as;

$$\frac{\partial L}{\partial x_i} = \frac{\partial F(x)}{\partial x_i} - \lambda^T \frac{\partial g(x)}{\partial x_i} - \mu^T \frac{\partial h(x)}{\partial x_i} \quad (58)$$

$$\mu^T h(x) = 0 \quad \mu_j \geq 0$$

In cases where it is unclear if a point satisfying the necessary conditions is a minimum, maximum, or otherwise, a set of second-order sufficient conditions may be applied for clarification (*Baker, et al.*, 2002). If the analytical representation of  $F(x)$  or the constraint set is not available, or not tractable, then numerical methods

may be applied to find an approximation to the solution of (57). The SQP method produces iterative estimates of the optimal parameter values and the Lagrange multipliers. As the numerical algorithm converges, these iterative estimates approach the optimal parameter values and Lagrange multipliers that would result from the analytical method Eq. (58), if it were applied. The primary computational components of a sequential quadratic program are responsible for the formation of an iterative locally quadratic approximation to the Lagrangian function, and a sufficient decrease line search of an augmented Lagrangian merit function [19],[20],[76]. An iterative quadratic approximation to the Lagrangian is given by,

$$L_q(x_k, \lambda_k, \mu_k) = L_q(x_{k-1}, \lambda_{k-1}, \mu_{k-1}) + \quad (59)$$

$$d_k^T \nabla \lambda^T g(x) - \mu^T h(x) L_q(x_{k-1}, \lambda_{k-1}, \mu_{k-1}) + \frac{1}{2} d_k^T B_k d_k$$

Where  $\nabla$  is the gradient operator (with respect to  $x$ ), and

$$d_x = x_k - x_{k-1} \quad (60)$$

And  $x_k$  and  $x_{k-1}$  are the values of the parameter vector  $x$  at the current iteration and the previous iteration, respectively. The second-order partial derivative, or Hessian, approximation matrix,  $B_k$  in Eq. (61), is generated by variable metric update equations [25]. The update that is typically applied is the Broyden-Fletcher-Goldfarb-Shanno (BFGS) update which was modified by *M.S. Bazaraa et al.*, 1993 as:

$$B_k = B_{k-1} - \frac{B_{k-1} s s^T}{s^T B_{k-1} s} + \frac{\eta \eta^T}{\eta^T s} \quad (61)$$

Where

$$s = x_{k-1} - x_{k-2} \quad (62)$$

$$\eta = \theta \omega - (1 - \theta) B_{k-1} s$$

$$\omega = \nabla L_q(x_{k-1}, \lambda_{k-1}, \mu_{k-1}) - \nabla L_q(x_{k-1}, \lambda_{k-1}, \mu_{k-1})$$

and

$$\theta = \begin{cases} 1 & \text{if } s^T \omega > 0.25 s^T B_{k-1} s \\ 0.8 & \\ \frac{0.8}{s^T B_{k-1} s} & \end{cases} \quad (63)$$

The quadratic approximation to the Lagrangian function is solved for the direction,  $d_k$ , in parameter

space that points in a minimizing direction of the quadratic. The variable metric matrix,  $B_k$ , must remain positive definite to ensure a bounded solution for the search direction,  $d_k$ . In practice, a positive definite  $B_k$  is maintained by the Levenberg-Marquardt method or by storing the variable metric updates in *Cholesky* decomposed form (*P.E. Gill et al.*, 1981). The positive definite state of  $B_k$  enables from Eq. (61) to be solved as a minimization problem. In a numerical setting, the quadratic approximation to the Lagrangian may be recast, through primal-dual relationships (*P.E. Gill et al.*, 1981), into the following quadratic sub problem with linearized constraints:

subject to:

$$\min_{d_k} F(x_{k-1}) + d_k^T \nabla F(x_{k-1}) + d_k^T B_k d_k \quad (64)$$

$$\text{subject to : } g(x_{k-1}) + d_k^T \nabla g(x_{k-1}) = 0$$

$$h(x_{k-1}) + d_k^T \nabla h(x_{k-1}) \geq 0$$

The maintenance of a positive definite  $B_k$  ensures that the local approximation given in Eq. (61) can be readily solved for the search direction,  $d_k$ , through standard convex quadratic programming methods (*Evangelos Zafiriou and Hung-Wen Chiou*, 1992) [24],[43]. In practice, other numerical techniques may be applied to prevent the linearized constraint approximations from completely closing off the feasible region *Fine T.L.*, 1999 and *Smith M.*, 1996. An active sets strategy (*Evangelos Zafiriou & Hung-Wen Chiou*, 1992) is also employed so that only the inequality constraints that are satisfied to within some small tolerance of an equality are included in the quadratic model, thereby reducing the overall computational effort [26],[32].

Following solution of the quadratic subproblem, a one-dimensional line search along the minimizing direction,  $d_k$ , is conducted. Another class of approximations to the Lagrangian (augmented Lagrangian merit functions) is typically used for this phase of the analysis. The centralized NNMPC techniques is used in our controller because it is control each parameters inside the system as shown in Fig. 6. The following merit Eq. (64) was used for this analysis as:

$$W(x_k, \lambda_k, \mu_k) = F(x_k) + \lambda_k^T g(x) + \mu_k^T h(x) \quad (65)$$

The iteration point,  $x_k$ , is determined by evaluating (64) at successive candidate points,  $x_k$ , until a sufficient

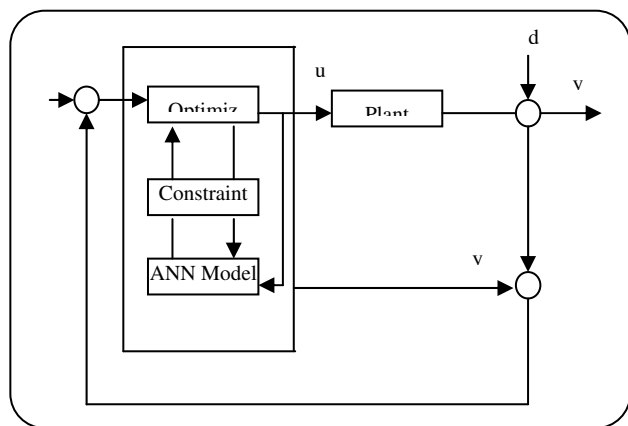


Fig. 6: The general structure of a nonlinear MPC.

decrease in the value of Eq. (65) is found. The candidate points are generated from the line search update Eqs. (65) and (66).

$$x_k^- = x_{k-1} + \alpha d_k \quad (66)$$

#### Neural Network Modeling

Before implementing the neural network based MPC a sufficiently accurate Artificial Neural Network (ANN) model of the polymerization system needs to be obtained. The steps used to obtain these models are outlined in the following section with some background of neural network itself[27],[36].

Basically, the ANNs are numerical structures inspired by the learning process in the human brain. They are constructed and used as alternative mathematical tools to solve a diversity of problems in the fields of system identification, forecasting, pattern recognition, classification, financial systems and many others (Huang & Mujumdar, 1993; Joaquim & Dente, 1997, Shaw et al., 1997; Baker & Richards, 2002). The interest in ANN as a mathematical modeling tool resulted in the consolidation of its theoretical background and the development of its underlying learning and optimization algorithms (Ang D.D. et al 1998; Huang, B et al,1993 ; Joaquim, A et al , 1997 and Shaw,et al ,1997).

Modeling and simulation of chemical processes is one of those research areas of interest that made use of ANN modeling techniques. The implementation of mechanistic models that rely on fundamental material and energy balances as well as empirical correlations involves a great deal of mathematical difficulties and in many instances lacks accuracy. Neural network-based modeling can be

used confidently as a substitute for such situations. This is due to the favorable features entailed in their use.

Among these features are; simplicity, fault and noise tolerance, robustness and ability for modelling nonlinear systems. The ANNs can be categorized in terms of its topology such as the multi-layer Feed Forward Neural Networks (FFNN), FeedBack Neural Networks (FBNN), Recurrent Neural Networks (RNN) and self-organized networks[34],[38]. In addition, they can be further categorized in terms of application, connection type and learning methods. FFNNs are the most commonly used type for function approximation. In this topology, the network is composed of one input layer, one output layer and a minimum of one hidden layer. The term feed forward describes the way in which the output of the FFNN is calculated from its input layer-by-layer throughout the network. In this case, the connections between network neurons do not form cycles. No matter how complex the network is, its building block utilizes a simple structure using the neurons. It performs a weighted sum of its inputs and calculates an output using certain predefined activation functions. Activation functions for the hidden units are needed to introduce the nonlinearity into the network. The Sigmoidal functions, such as logistic and tanh, and the Gaussian function, are the most common choices for the activation functions. The number of neurons and the way in which the neurons are interconnected defines the neural system architecture. The network is fed with a set of input-output pairs and trained to reproduce the outputs. Adjusting the neurons weights using an optimization algorithm to minimize the quadratic error between observed data and computed outputs do the training. A good reference on the FFNN and their applications is given by Fine, 1999.

Input-target training data are usually pretreated in order to improve the numerical condition for the optimization problem and for better behavior of the training process. Thus, the data are normally divided into three subsets; training, validation and testing subsets. The training subset data are used to accomplish the network learning and fit the network weights by minimizing an appropriate error function. It refers to the method for computing the gradient of the error function with respect to the weights for a feed forward network. Evaluating the error function using the validation subset data, independently, then compares the performance of the network. The testing subset data are then used to measure

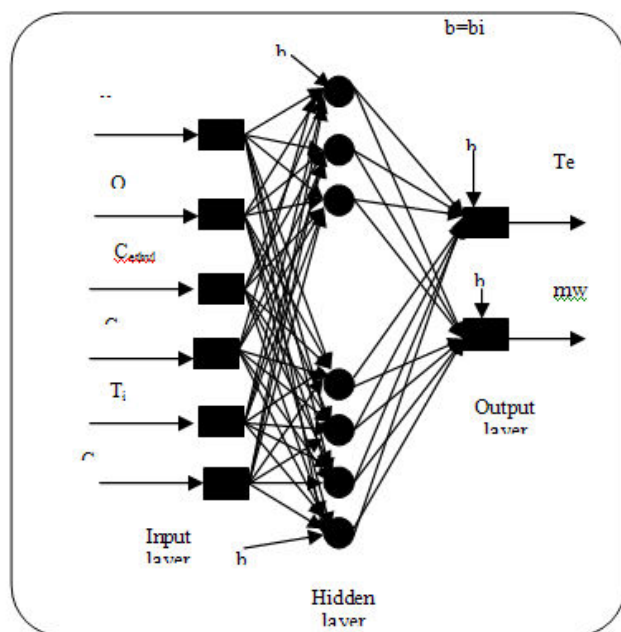


Fig. 7: Three layer feed forward neural network

the generalization of the network (i.e. how accurately the network predicts targets for inputs that are not in the training set). Improperly trained neural networks may suffer from either under fitting or over fitting. The former describes the condition when a network that is not sufficiently complex fails to fully detect the signal in a complicated data set. On the other hand, the latter condition occurs when a network that is too complex may fit the noise, in addition to the exiting signal (Smith, 1996).

Selecting network structure is a crucial step in the overall design of NNs. The structure must be optimized to reduce computer processing, achieve good performance and avoid over fitting. Experience in using ANN for function approximation revealed that any nonlinear function can be approximated by a three layer ANN structure. The selection of the best number of hidden units depends on many factors. The size of the training set, amount of noise in the targets, complexity of the sought function to be modeled, type of activation functions used and the training algorithm all have interacting effects on the sizes of the hidden layers. Details of training a neural network can be found in M.S. Bazaraa *et al.*, 1993. The finally trained ANNs represent the general relations linking ANN inputs to its output for the modified mathematical model of the fluidized bed for the gas phase olefin polymerization reactor.

### Neural Network modeling of Polymerization System

The data used for training the neural network model was generated from the non linear model of the system (hammed *et al.*,2008. Step tests data were generated in simulation for the model with change in inputs values for superficial velocity and catalyst flow rate as shown in Fig. (11) and (12).

The inputs corresponding ranges for all gases mole fraction concentrations were form with other superficial velocity were from (0.1 to 0.75) and for temperature input range from (300-395 K). The selected ranges cover the whole spectrum of model system including of flooding conditions and both outlet emulsion temperature and molecular weight. Data sets were divided into three subsets; training, validation and testing.

The neural network structure was selected based on testing different network configurations that vary in terms of structure and simulation parameters. The criterion for network structure selection is based on its simplicity, performance, and accuracy of model prediction. The finally selected network contained 1 hidden layer with 8 neurons. The activation function used in the hidden layer is the tanh function because it is more suitable for the highly non linear system, while the output layer contains linear neurons. The inputs and outputs to the network are as shown in Fig. 7.

Fig. 7 six input with the time -two outputs data sets were generated by introducing random steps in the manipulated variables at a sampling time 3h and collecting the outputs emulsion temperature  $T_e$  and molecular weight MW.

So, we can specify the inputs as ( $u_o(t,t-1,\dots,t-n+1)$ ),  $Q_c(t,t-1,\dots,t-n+1)$ , Cethylene ( $t,t-1,\dots,t-n+1$ ), Cbutene ( $t, t-1,\dots,t-n+1$ ),  $T_{in}$  ( $t, t-1,\dots,t-n+1$ ) and Chydrogen ( $t, t-1,\dots,t-n+1$ ) and outputs ( $T_e$  ( $t, t-1,\dots,t-m+1$ ) and MW ( $t, t-1,\dots,t-m+1$ )). The neural network shown in Figs. 4.4 to 4.6 is in the process of being trained using a feed forward neural net work.

The inputs and target are represented with the interval value [-1, 1]. This would make the neural network training more efficient. Network training was accomplished by manipulating its weights and biases to achieve certain performance criteria. This was done by using an optimization algorithm for searches for network parameters that minimize the predicative error described by Eq. (53).

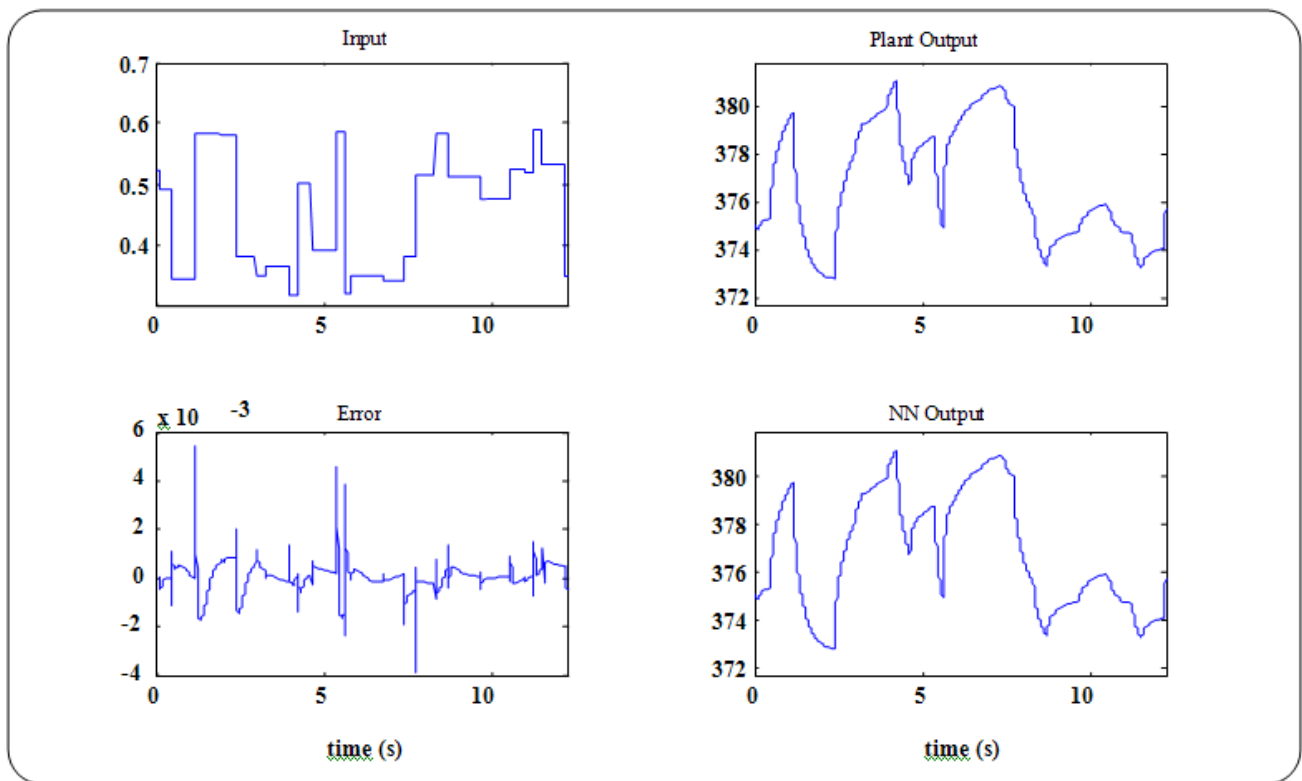


Fig. 8: Input-output training set for molecular weight ANN predictions.

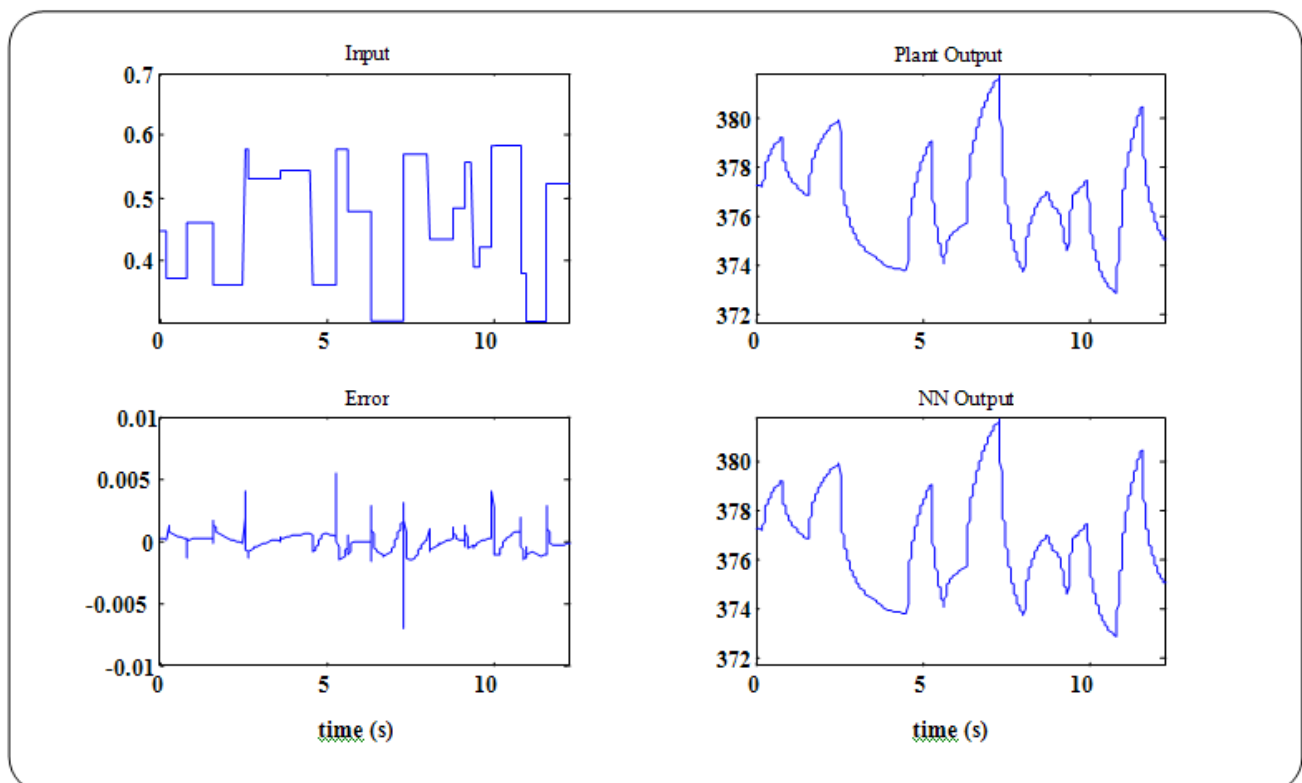


Fig. 9: Input-output training set for emulsion temperature ANN predictions.

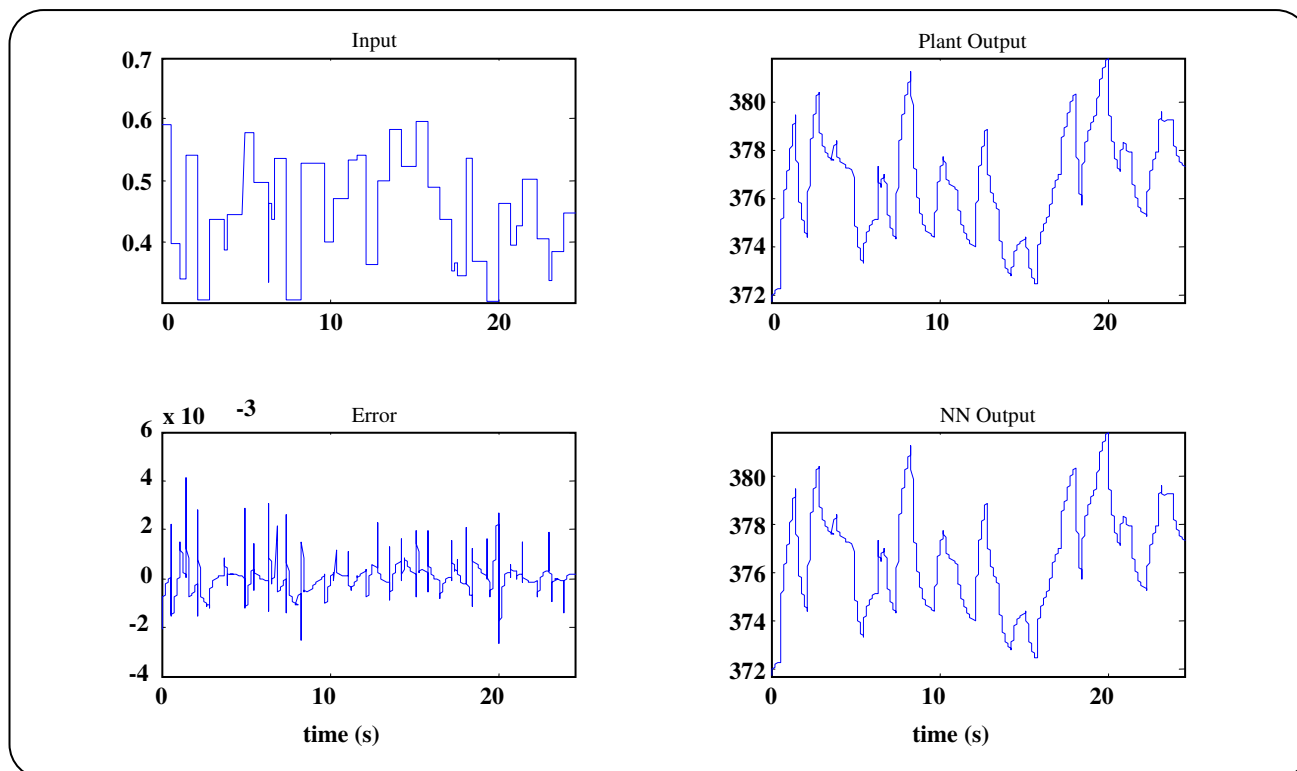


Fig. 10: Analyses for validation data

In "Reaction Kinetics" section, it has been shown that the fluidized bed polyethylene process is highly nonlinear, especially with excitations in the superficial gas velocity and that the effect of nonlinearity is more pronounced on emulsion temperature and molecular weight than the catalyst flow rate but both these inputs have big effect on the system. The central control system for NMPC can be controlled by each variables input inside the system. This system is affected by four disturbances, namely concentration of ethylene (Cethylene), concentration of butane (Cbutene), concentration of hydrogen (Chydrogen) and temperature input  $T_{in}$ . This configuration is adopted in this study.

In order to facilitate the use of the control algorithms to be studied, a neural network model of the fluidize process under consideration is constructed. This is achieved by generation a set of input-output network training data using the developed mechanistic model. Used two networks for the two set points emulsion temperature and molecular weight. The Levenberg-Marquardt Back Propagation (LMBP) optimization algorithm was used for network training. This algorithm gives good performance with an average error for

the two networks (uo-Te) and (Qc-MW) was  $1 \times 10^{-8}$ . The achieved networks then were validated and tested using the data subsets previously generated from the model. A comparison of both modeled and network-predicted outputs for both phases is shown in the form of the error profiles in Figs. 8, 9, and 10. These Figures indicate low errors even under severe process excitations.

SQP approach utilizing the Quasi-Newton method with a conjugate gradient algorithm was used for the nonlinear constrained optimization in NMPC as Has been previously explained in "SQP" section 4.2 and Fig. 6.

#### Simulation and Results

The neural network models obtained as for training in the previous section were utilized in model predictive Schemes as described in previous section. Simulation studies including set point tracking and disturbance rejection studies such as changes in hydrogen, butene, ethylene concentrations, inlet temperature, superficial velocity and catalyst flow rate were done in this work.

For the case of constrained control, the MPC was able to drive the system dynamics to the desired values effectively without violating the limitations assigned for

**Table 5: Dynamic response characteristics for a set point of emulsion temperature.**

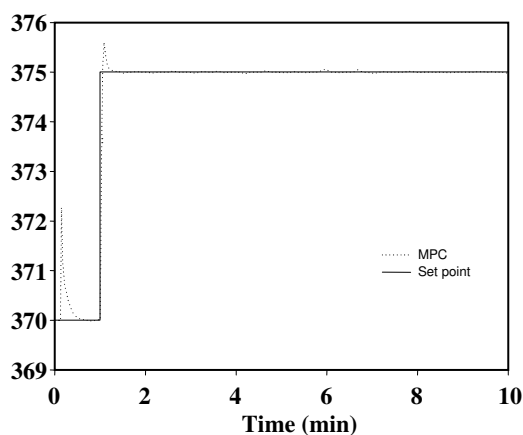
Tuning Method	LOOP	Rise time (min)	Overshoot	Settling time IAE (min)	
MPC	$U_o.T_e$	1.23	-	1.255	0.013
	$Q_c.MW$	1.35	-	1.435	0.054
PID	$U_o.T_e$	1.7	-	1.555	2.09
	$Q_c.MW$	1.86	-	1.89	2.34

**Table 6: Integrated absolute error for set point and disturbance rejection of the emulsion temperature closed loop using the NN-MPC as compared to the PID controller.**

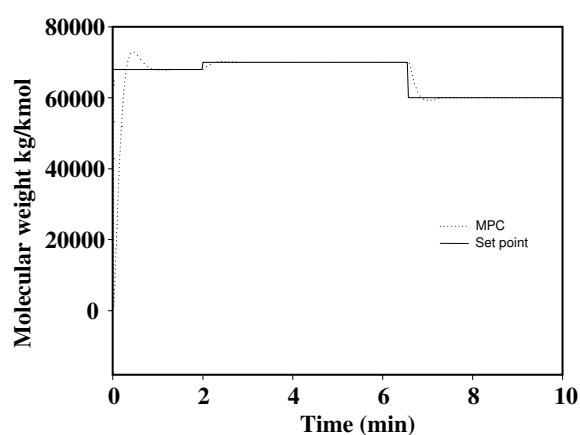
Controller	Set point IAE	Disturbance in hydrogen concentration IAE	Disturbance in ethylene concentration IAE	Disturbance in butane concentration IAE	Disturbance in inlet temperature IAE
MPC	0.045	0.0087	0.0106	0.096	0.0128
PID	0.15	0.091	0.109	0.103	0.130

**Table 7: Integrated absolute error for set point and disturbance rejection of the molecular weight closed loop using the NN-MPC as compared to the PID controller.**

Controller	Set point IAE	Disturbance in hydrogen concentration IAE	Disturbance in ethylene concentration IAE	Disturbance in butane concentration IAE	Disturbance in inlet temperature IAE
MPC	0.1926	0.383	0.2788	0.4382	0.2042
PID	2.255	3.056	2.386	3.755	2.401

**Fig. 11: MPC controller response for set point tracking study of superficial gas velocity on set point.**

the manipulated variables. Of course there were some little differences between the two controllers in terms of set point tracking time and damping of response, but in terms of control criteria, the constrained case was acceptable and doesn't have much deviation from the unconstrained one. The characteristics of the dynamic responses are calculated and given in Table 5. The missing values in the table indicate no value or an inapplicable measure.

**Fig. 12: MPC controller for set point tracking study of catalyst flow rate on set point.**

The Integral Absolute Errors (IAE) of the process responses are shown in Tables 6 and 7.

From the response characteristics of the different tuning algorithms the following can be noticed:

Effects of disturbances on the two outputs are shown in Tables 6 and 7 a good idea about performance of MPC controller.

Figs. 11 and 12 show the neural-network based

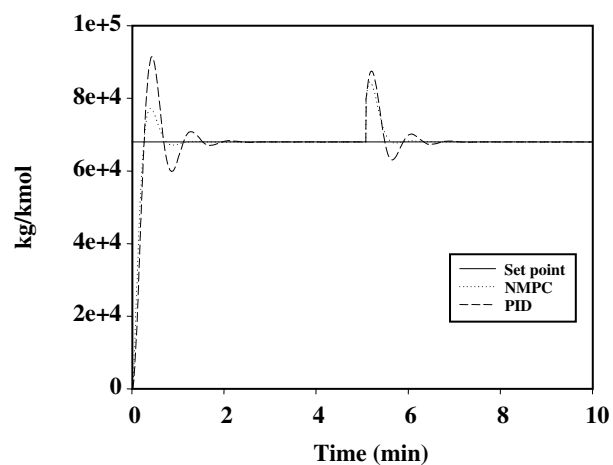
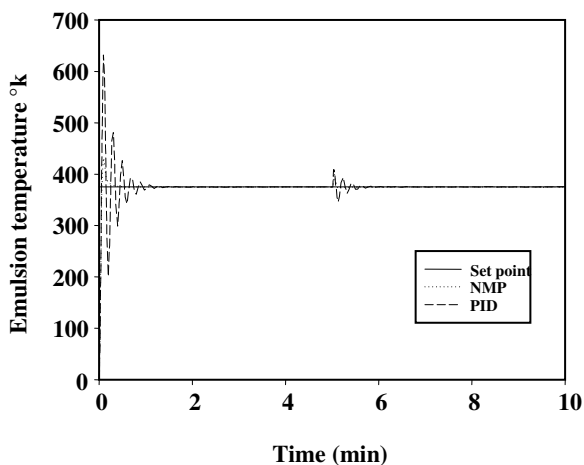


Fig. 13: MPC controller for disturbance hydrogen concentration on set point.

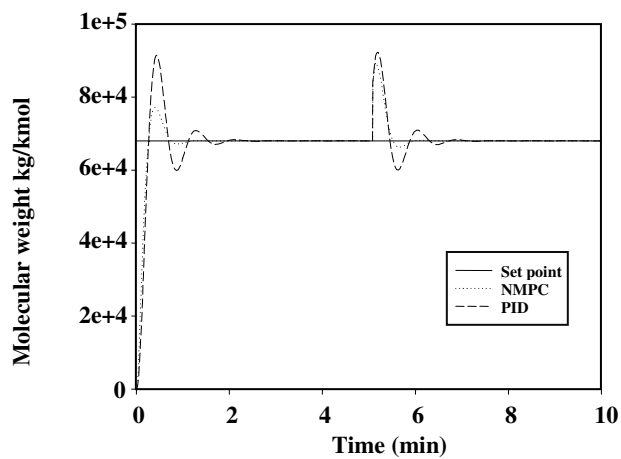
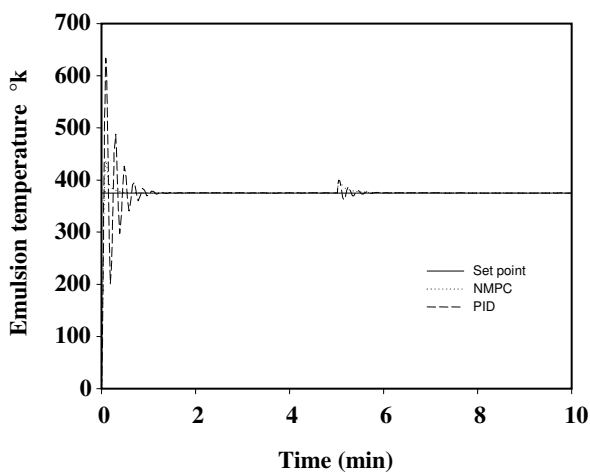


Fig. 14: MPC controller for disturbance of butene concentration disturbance on set point.

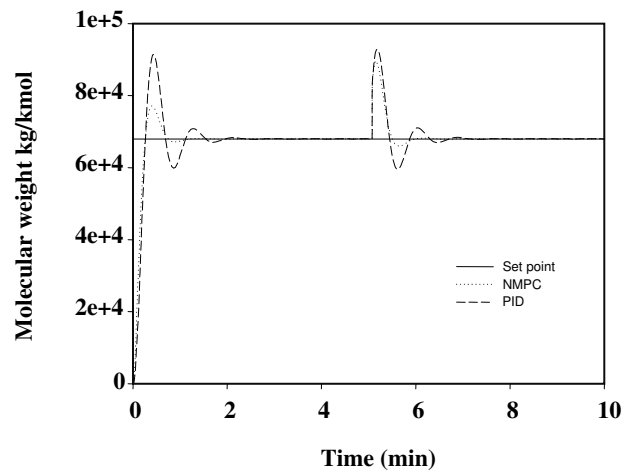
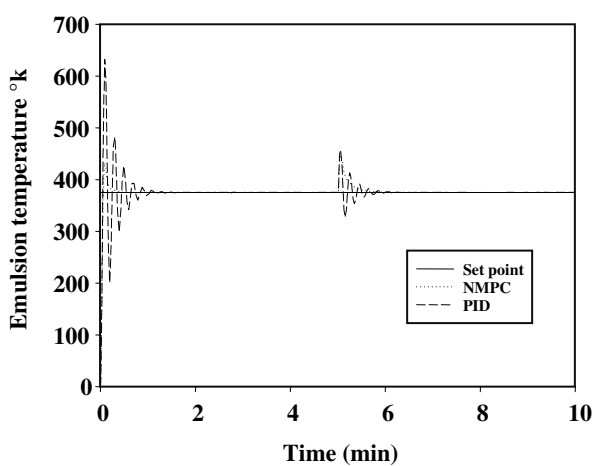


Fig. 15: MPC controller for disturbance of ethylene concentration on set point

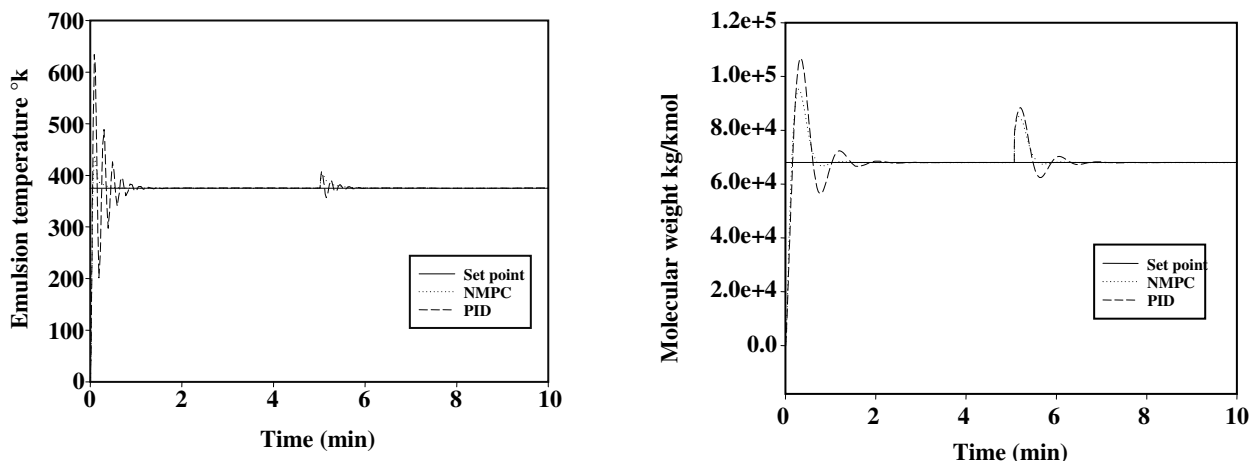


Fig. 16: MPC controller for disturbance of inlet temperature on set point.

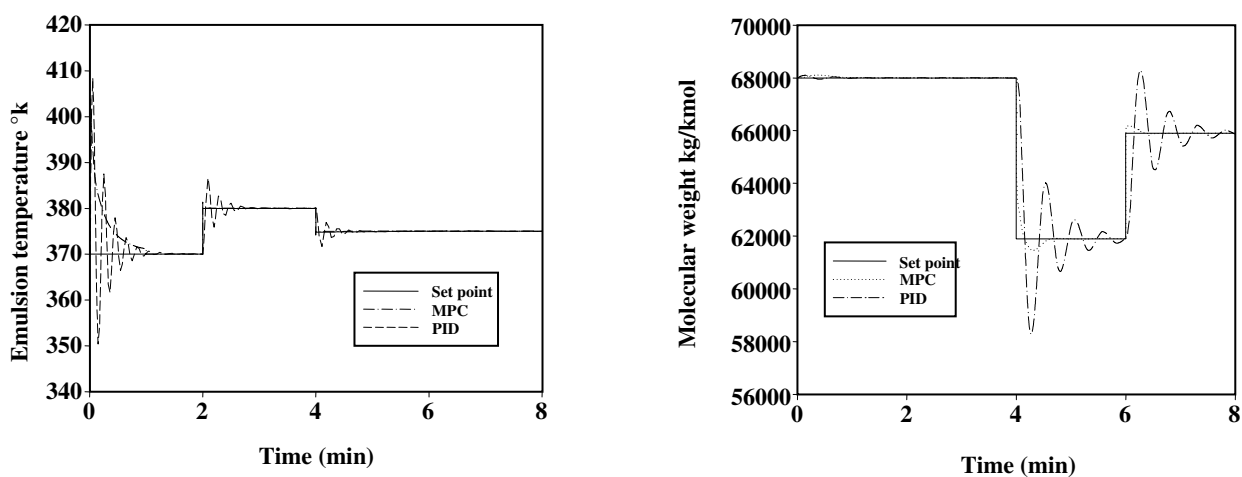


Fig. 17: Response for set point tracking studies - MPC comparison with PID controllers for superficial velocity rejection study.

predictive controller performance for set point tracking without any oscillations in both cases. The results show that a fast rise time was achieved, with a very small overshoot for both loops.

The disturbances introduced are changes in the initial hydrogen, butene, ethylene concentrations and inlet temperature respectively shown in Figs. 13 to 16 the behavior of MPC is very active and smooth without any oscillations. From Figs. 13 to 16 PID and MPC controllers for disturbance of hydrogen, butene, ethylene concentrations and inlet temperature respectively rejection study on set point show that PID controller is characterized with slightly longer settling times control with a digressive action oscillations before achieving the set point with a higher overshoots compare to MPC as shown in Fig. 17.

From these results it can be inferred that the behavior of comparison of PID and MPC controllers for set point shown in Fig. 17 PID controller is characterized with slightly longer settling times control action with oscillations before achieving the set point with a higher overshoots compare to MPC.

## CONCLUSIONS

The trained neural network was capable of capturing the fluidized-bed process dynamics with high prediction efficiency and thus can be used in control applications where the process exhibits high nonlinear dynamics such as the fluidized bed process. The performance of the NN-MPC for the set-point tracking and disturbance case was excellent in forcing the process output variables to their

target values smoothly and within reasonable speed compare to PID because it is optimizer control system depends on SQP one of the best non linear optimization methods. The controller showed stable behavior for the whole spectrum of excitations in the output variable. Therefore, we prefer to use decentralize NMPC controller especially for complex industrial processes where controller computing time is important.

### Nomenclature

$A_1$	Cross-sectional area of the bed, $\text{cm}^2$
Ar	Archimedes number $[= d_p^3 \rho_g (\rho_s - \rho_g) g / \mu^2]$
$A_{sf}^k$	Fraction of metal that can form "k" catalyst active
$A_B$	Cross sectional area of bubble phase, $\text{m}^2$
$C_d^k$	Concentration of deactivated catalyst active sites, $\text{mol}/\text{cm}^3$
$C_{pg}$	Specific heat capacity of gaseous stream, $\text{cal}/\text{g}/\text{K}$
$C_{PMi}$	Specific heat of "I" monomer, $\text{cal}/\text{mol}/\text{K}$
$C_{p,pol}$	Specific heat capacity of polymer product, $\text{cal}/\text{g}/\text{K}$
$C_{A,S}$	Adsorbed surface concentration of A in $\text{kmol}/\text{kg}$ catalyst
$C_{B,S}$	Product desorption of B in $\text{kmol}/\text{kg}$ .catalyst
$C_B$	Product concentration $\text{kmol}/\text{kg}$ .catalyst
$C_V$	Vacant molar concentration sites $\text{kmol}/\text{kg}$ .catalyst
$C_{cat}$	Mass fraction of catalyst in the solid phase
$C_{AB}$	Concentration of monomer gas in bubble phase $\text{kg}/\text{m}^3$
$C_{AC}$	Concentration of monomer gas in cloud phase $\text{kg}/\text{m}^3$
$C_{Ae}$	Concentration of emulsion phase $\text{kg}/\text{m}^3$
$d_{bm}$	Maximum stable bubble size, cm
$d_p$	Particle diameter, cm
$d_b$	Bubble diameter, cm
$D_g$	Gas self-diffusion coefficient, $\text{cm}^2/\text{s}$
$D_n^k$	Concentration of "dead" copolymer chains, $\text{mol}/\text{cm}^3$
$D_{bed}$	Bed diameter, m
h	Random bed height, m
H	Total bed height, cm

$H_{mf}$	Bed height at minimum fluidization conditions, m
$H_{bc}$	Bubble to cloud heat transfer coefficient, $\text{cal}/\text{m}^3/\text{s}/\text{K}$
$H_{ce}$	Cloud to emulsion heat transfer coefficient, $\text{cal}/\text{m}^3/\text{s}/\text{K}$
$H_{be}$	Bubble to emulsion heat transfer coefficient, $\text{cal}/\text{m}^3/\text{s}/\text{K}$
$[H_2]$	Hydrogen concentration, $\text{mol}/\text{m}^3$
$k_g$	Gas thermal conductivity, $\text{J}/\text{m}/\text{s}/\text{K}$
$K_{bc}$	Bubble to cloud mass transfer coefficient, $1/\text{s}$
$K_{ce}$	Cloud to emulsion mass transfer coefficient, $1/\text{s}$
$K_{be}$	Bubble to emulsion mass transfer coefficient, $1/\text{s}$
$k_i$	Rate constant of reaction, $1/\text{s}$
$k_A$	Thermal conductivity between layers of catalyst particles, $\text{J}/\text{m}^2/\text{s}/\text{K}$
$k^n$	Rate constant of spontaneous reaction $1/\text{s}$
$k^f$	Rate constant of chain transfer $1/\text{s}$
$K^h$	Rate constant of chain transfer to hydrogen $1/\text{s}$
MFI	Melt flow index of polymer (g per 10 min)
$[M_e]$	Active metal concentration, $\text{mol Me}/\text{m}^3$
$[M_i]$	"I" monomer concentration, $\text{mol Me}/\text{m}^3$
$P_A$	Partial pressure of A in gas phase
$P^O$	Potential active sites $\text{kmol}/\text{m}^3$
$P_o$	Active sites concentration $\text{kmol}/\text{m}^3$
$u_{mf}$	Minimum fluidization velocity, $\text{m}/\text{s}$
$u_e$	Emulsion gas velocity, $\text{m}/\text{s}$
$S_P^K$	Concentration of potential "k" catalyst active sites, $\text{mol}/\text{m}^3$
$Q_0$	Volumetric product removal rate, $\text{m}^3/\text{s}$
V	Volume, $\text{m}^3$
T	Temperature, K
$T_b$	Temperature in the bubble phase K
$T_{ref}$	Reference temperature K
$T_e$	Emulsion phase temperature K
$T_w$	Wall temperature K
$T_{fs}$	Temperature of inlet catalyst K
$T_f$	Temperature of the feed gas K
$r_a$	Rate expression for the active sites $\text{kmol}/\text{kg}$ .catalyst
$R_{\mu n,i}^k$	Rate expression for live moments
$R_{\nu n,i}^k$	Rate expression for dead moments
$R_X^K$	Reaction rate of species X at "k" catalyst activesites, $\text{mol}/\text{m}^3/\text{s}$
r	Radius, m
Z	Bed height, m

**Greek letters**

$\mu_0^k$	Live polymer zero
$\mu_1^k$	Live polymer
$\mu_2^k$	Live polymer
$v_0^k$	Dead polymer
$v_1^k$	Dead polymer
$v_2^k$	Dead polymer
$\delta^*$	Fraction of fluidized-bed consisting of bubbles
$\mu_g$	Viscosity of gas, g/cm/s
$\pi$	Constant ratio
$\varepsilon$	Void fraction of the bed at minimum fluidized velocity
$\delta_b$	Bubble phase volume fraction
$\rho_s$	Solid density, kg/m <sup>3</sup>
$\Delta H_{rxn}$	Heat of reaction, kJ/kg
$I_k$	Objective function
$\xi$	Suitable large number
$\mu$	Lagrange multiplier vector
$\lambda$	Lagrange multiplier vector
$\alpha$	Ratio between weak to bubble volume

**Number**

1	Monomer gas ethylene
2	Mmonomer gas butane

Received : July 12, 2009 ; Accepted : Apr. 18, 2012

**REFERENCES**

- [1] Ahmmed S. Ibrehem, Mohamed Azlan Hussain, Nayef Mohamed Ghasem, Mathematical Model and Advanced Control for Gas Phase Olefin Polymerization in Fluidized-Bed Catalytic Reactors, *Chinese Journal of Chemical Engineering*, **16**(1), p. 84 (2007).
- [2] Helal A.M., Elnashaie S.S., Numerical Construction of Bifurcation Diagrams for Non-Linear Complex Reaction Networks in Catalytic Reactors, *Computers & Chemical Engineering*, **14**(6), p. 691 (1990).
- [3] Antonio Flores-Tlacuahuac, Lorenz T. Biegler, A Robust and Efficient Mixed-integer Non-Linear Dynamic Optimization Approach for Simultaneous Design and Control, *Computer Aided Chemical Engineering*, **20**(1), p. 67 (2005).
- [4] Kiashemshaki A., Mostoufi N., Pourmahdian S, Sotudeh-GharebaghR., Two phase Modeling of a Gas Phase Polyethylene Fluidized Bed Reactor, *Chemical Engineering Science*, **61**, p. 3997 (2006).
- [5] Aswin N. Venkat, P. Vijaysai and Ravindra D. Gudi, Identification of Complex Nonlinear Processes Based on Fuzzy Decomposition of the Steady State Space, *Electronic Journal of Biotechnology*, **10**(4), (2007).
- [6] Baker B.D., Richards C.E., Exploratory Application of Systems Dynamics Modeling to School Finance Policy, *Journal of Education Finance*, **27**(3), p. 857 (2002).
- [7] Biegler L., Improved Infeasible Path Optimizer for Sequential Modular Simulators-I: The Interface, *Computers and Chemical Engineering*, **9**(3), p. 245 (1985).
- [8] Bassam Alhamad, Jose A. Romagnoli, Vincent G. Gomes, On-Line Multi-Variable Predictive Control of Molar Mass and Particle Size Distributions in Free-Radical Emulsion Copolymerization, *Chemical Engineering Science*, **60**(23), p. 6596 (2005).
- [9] Babatunde A. Ogunnaike, Kapil Mukati, An Alternative Structure for Next Generation Regulatory Controllers : Part I: Basic Theory for Design, Development and Implementation, *Journal of Process Control*, **16**(5), p. 499 (2006).
- [10] Chatzidoukas C., Perkins J.D., Pistikopoulos E.N., Kiparissides C., Optimal-Grade Ransition and Selection of Closed-Loop Controllers in a Gas-Phase Olefin Polymerization Fluidized Bed Reactor, *Chemical Engineering Science*, **58**, p. 3643 (2003).
- [11] Chiaki Kuroda, Jinyoung Kim, Neural Network Modeling of Temperature Behavior in an Exothermic Polymerization Process, *Neurocomputing*, **43**(1-4), p. 77 (2002).
- [12] Charles D., Francis J. Doyle, Modeling of Particle Size Distribution in Emulsion co-Polymerization: Comparison with Experimental Data and Parametric Sensitivity Studies, *Computers & Chemical Engineering*, **26**(7-8), p. 1133 (2002).
- [13] Ang D.D., Pham Ngoc Dinh A., Thanh D.N., Regularization of an Inverse Two-Phase Stefan Problem, **34**(5), p. 719 (1998).
- [14] Dennis Van Hessem, Okko Bosgra, Stochastic Closed-Loop Model Predictive Control of Continuous Nonlinear Chemical Processes, *Journal of Process Control*, **16**(3), p. 225 (2006).

- [15] Del Vecchio D., Petit N., Boundary Control for An Industrial Under-Actuated Tubular Chemical Reactor, *Journal of Process Control*, **15**(7), p. 771 (2005).
- [16] Dulce C.M. Silva, Nuno M.C. Oliveira, Optimization and Nonlinear Model Predictive Control of Batch Polymerization Systems, *Computers & Chemical Engineering*, **26**(4-5), p. 649 (2002).
- [17] Baker E.L., "Modeling and Optimization of Shaped Charge Liner Collapse and Jet Formation", Ph.D. Dissertation, Washington State University, Pullman, Washington, (1992).
- [18] Fine T.L., "Feed Forward Neural Network Methodology", Springer, New York (1999).
- [19] Francis J. Doyle, III, Christopher A. Harrison, Timothy J. Crowley, Hybrid Model-Based Approach to Batch-to-Batch Control of Particle Size Distribution in Emulsion Polymerization, *Computers & Chemical Engineering*, **27**(8-9), p. 1153 (2003).
- [20] Mourue G., Dochain D., Wertz V., Descamps P., Identification and Control of An Industrial Polymerisation Reactor, *Control Engineering Practice*, **12**(7), p. 909 (2004).
- [21] Gangadhar Gattu, Evangelos Zafiriou, A Methodology for on-Line Setpoint Modification for Batch Reactor Control in the Presence of Modeling Error, *Chemical Engineering Journal*, **75**(1), p. 21 (1999).
- [22] Ravi Srinivas G., Arkun Y., Joseph Schork F., Estimation and Control of an  $\alpha$ -Olefin Polymerization Reactor, *Journal of Process Control*, **5**(5), p. 303 (1995).
- [23] Hatzantonis H., Yiannoulakis H., Yiagopoulos A., Kiparissides C., Recent Developments in Modeling Gas-Phase Catalyst Olefin Polymerization Fluidized Bed Reactor: The Effect of Bubble Size Variation on the Reactor's Performance, *Chemical Engineering Science*, **5**, p. 3237 (2000).
- [24] Huang B., Mujumdar A.S., Use of Neural Network to Predict Industrial Dryer Performance, *Drying Technology*, **3**, p. 525 (1993).
- [25] Hiroya Seki, Morimasa Ogawa, Satoshi Ooyama, Kouji Akamatsu, Masahiro Ohshima, Wang Yang, Industrial Application of a Nonlinear Model Predictive Control to Polymerization Reactors, *Control Engineering Practice*, **9**(8), p. 819 (2001).
- [26] Joachim Horn, Trajectory Tracking of a Batch Polymerization Reactor Based on Input-Output-Linearization of a Neural Process Model, *Computers & Chemical Engineering*, **25**(11-12), p. 1561 (2001).
- [27] Joaquim A., Dente R., Vilela mendes, Characteristic Functions and Process Identification by Neural Networks, *Neural Networks*, **10**, p. 1465 (1997).
- [28] Jesus Flores-Cerrillo, John F. MacGregor, Latent Variable MPC for Trajectory Tracking in Batch Processes, *Journal of Process Control*, **15**(6), p. 651 (2005).
- [29] Choi K.Y., Ray W.H., The Dynamic Behaviour of Fluidized Bed Reactors for Solid Catalyzed Gas Phase Olefin Polymerization, *Chem. Eng. Sci.*, **40**, p. 2261 (1985).
- [30] Kenneth R. Harris, Ahmet Palazolu, Control of Nonlinear Processes Using Functional Expansion Models, *Computers & Chemical Engineering*, **27**(8-9), p. 1061 (2003).
- [31] Mc Auley Tousain, R.L. Bosgra, O.H., Efficient Dynamic Optimization for Nonlinear Model Predictive Control-Application to a High-Density Poly-Ethylene Grade Change Problem, Decision and Control, "Proceedings of the 39th IEEE Conference", Vol. 1, pp. 760-765 (2000).
- [32] Powell M.J.D., in "Numerical Analysis, Proceedings of the Biennial Conference Held at Dundee", G.A. Watson eds., Lecture Notes in Mathematics, Vol. 630, Springer-Verlag, Berlin, New York, 1978, p. 144 (1977).
- [33] Bazaraa M.S., Sherali H.D., Shetty C.M., "Nonlinear Programming: Theory and Algorithms", 2nd edition, John Wiley & Sons, Inc., New York, (1993).
- [34] Hussain M.A., Shafiur Rahman M., Ng C.W., Prediction of Pores Formation (Porosity) in Foods During Drying: Generic Models by the Use of Hybrid Neural Network, *Journal of Food Engineering*, **51**(3), p. 239 (2002).
- [35] Mourad M., Hémati M., Laguérie Ming C., Drying of Maize in a Fluidized Bed: II: A Kinetic Model, of, Drying, *Chemical Engineering Journal and the Biochemical Engineering Journal*, **60**, p. 39 (1995).

- [36] Morimasa Ogawa, Masahiro Ohshima, Koji Morinaga, Fuminao Watanabe, Quality Inferential Control of an Industrial High Density Polyethylene Process, *Journal of Process Control*, **9**(1), p. 51 (1999).
- [37] Mourad M., He´ mati M., Lague´ rieMing C., Drying of Maize in a Fluidized Bed: II: a Kinetic Model of Drying, *The Chemical Engineering Journal and the Biochemical Engineering Journal*, **60** (1–3, 12), p. 39 (1995).
- [38] Mariano Asteasuain, Alberto Bandoni, Claudia Sarmoria, Adriana Brandolin, Simultaneous Process and Control System Design for Grade Transition in Styrene Polymerization, *Chemical Engineering Science*, **61**(10), p. 3362 (2006).
- [39] Mahmood Alizadeh, Navid Mostoufi, Saeed Pourmahdian, Rahmat Sotudeh-Gharebagh, Modeling of Fluidized Bed Reactor of Ethylene Polymerization, *Chemical Engineering Journal*, **97**, p. 27 (2004).
- [40] Nayef Mohamed Ghasem, Mohd Zaki Sulaiman and Mohd Azlan Hussain, Simulation, Optimization and Parametric Studies of a Solid Catalyzed Gas Phase Ethylene Polymerization Fluidized Bed Reactor, *Journal of Chemical Eng. of Japan*, **38** p. 171 (2005).
- [41] Abel O., Helbig A., Marquardt W., Zwick H., Daszkowski T., Productivity Optimization of An Industrial Semi-Batch Polymerization Reactor Under Safety Constraints, *Journal of Process Control*, **10**(4), p. 351 (2000).
- [42] Patwardhan R., Lakshminaraynan S., Shah S., Constrained nonlinear MPC Using Hammerstein and Wiener Models: PLS framework, *AIChE Journal*, **44**(7), p. 1611 (1998).
- [43] Gill P.E., Murry W., Wright M.H., "Practical Optimization", Academic Press, New York, 1981.
- [44] Evangelhos Zafiriou and Hung-Wen Chiou, On the Effect of Constraint Softening on the Stability and Performance of Model Predictive Controllers, *AIChE*, **1**, p. 6 (1992).
- [45] Roos. Sala, F. Valz-Gris and L. Zanderighi, A Fluid-Dynamic Study of a Continuous Polymerisation Reactor, *Chemical Engineering Science*, **29**, p. 2205 (1974).
- [46] Reddy B.V., Nag P.K., Axial and Radial Heat Transfer Studies in a Circulating Fluidized Bed, *International Journal of Energy Research*, **21**, p. 1109 (1997).
- [47] Rao C.V., Wright S.J., Rawlings J.B., Application of Interior-Point Methods to Model Predictive Control, *Journal of Optimization Theory and Applications*, **99**(3), p. 723 (1998).
- [48] Sala R., Valz-Gris F., Zanderighi L., A Fluid-Dynamic Study of a Continuous Polymerisation Reactor, *Chemical Engineering Science*, **29**, p. 2205 (1974).
- [49] Zeman R.J., Amundson N.R., Continuous Polymerization Models-Part II : Batch Reactor Polymerization, *Chemical Engineering Science*, **20**, p. 637 (1965).
- [50] Roberto Lemoine-Nava, Antonio Flores-Tlacuahuac, Enrique Sald´ıvar-Guerra, Non-linear Bifurcation Analysis of the Living Nitroxide-Mediated Radical Polymerization of Styrene in a CSTR, *Chemical Engineering Science*, **61**(2), p. 370 (2006).
- [51] Shaw A.M., Doyle F.J., Schwaber J.S., A Dynamic Neural Network Approach to Nonlinear Process Modeling, *Computers and Chemical Engineering*, **21**, p. 371 (1997).
- [52] Smith M., "Neural Networks for Statistical Modeling", International Thomson Computer Press, Boston (1996).
- [53] Sablani S.S., A Neural Network Approach for Non-Iterative Calculation of Heat Transfer Coefficient in Fluid-Particle Systems, *Chem. Eng. Process.*, **40**, p. 363 (2001).
- [54] Shahaf G., Marom S., Learning in Networks of Cortical Neurons, *Journal of Neuroscience*, **21**, p. 8782 (2001).
- [55] Shaw A.M., Doyle F.J., Schwaber J.S I., A Dynamic Neural Network Approach to Nonlinear Process Modeling, *Computers and Chemical Engineering*, **21**, p. 371 (1997).
- [56] Sit S.P., Grace J.R., Effect of Bubble Interaction on Interphase Mass Transfer in Gas Fluidized Beds, *Chemical Engineering Science*, **36**, p. 327 (1981).
- [57] Smith, "Neural Networks for Statistical Modeling", International Thomson Computer Press, Boston, (1996).
- [58] Sreekanth S.S., Ramaswamy H.S., Sablani S.S., Prasher S.O., A Neural Network Approach for Evaluation of Surface Heat Transfer Coefficient, *Journal of Food Processing and Preservation*, **23**(4), p. 329 (1999).

- [59] Sang, Hyun, Neural Network Modeling of Temperature Behavior in An Exothermic Polymerization Process, *Neurocomputing*, **43**(1-4), p. 77 (2002).
- [60] Simant R. Upreti, Baranitharan S. Sundaram, Ali Lohi, Optimal Control Determination of MMA Polymerization in Non-Isothermal Batch Reactor Using Bifunctional Initiator, *European Polymer Journal*, **41**(12), p. 2893 (2005).
- [61] Thomas, Francis, An Anti-Windup Scheme for Multivariable Nonlinear Systems, *Journal of Process Control*, **14**(8), p. 899 (2004).
- [62] Tarmy B.I., Coulaloglou, Industrial View of Gas/Liquid/Solid Reactor Development, *Chemical Engineering Science*, **47**, p. 3231 (1992).
- [63] Stephen Whitaker, "Handbook of Heat and Mass Transfer", vol.3, Catalyst, Kinetics, and Reactor Engineering, Ch. 26, p. 1061 (1989).
- [64] Tabis B., Essekkat A., Three-Phase Multi-Compartment Model for Fluidized-Bed Catalytic Reactor. Autothermicity and Multiplicity of Steady States, *Chem.Eng.Sci.*, **47**(2), p. 407 (1992).
- [65] Toomey R.D., Johnstone, Gaseous Fluidization of Solid Particles, *Chemical Engineering Progress*, **48**, p. 220 (1952).
- [66] Wolf J.A., Moyer J.T., Lazarewicz M.T., Contreras D., Benoit-Marand M., O'Donnell P., Finkel L.H., Neuron or Other Electrically Excitable Cell, *Physical Science Journal*, **1**(3), p. 13 (2005).
- [67] Wei, Danial, "Control Relevant Model Reduction of Voltra Series Models, Department of Chemical, Bio and Materials Engineering and Control Systems Engineering", Arizona State University, USA, (1997).
- [68] Werther, Modeling and Scale-Up of Industrial Fluidized Bed Reactors, *Chemical Engineering Science*, **35**(1-2), p. 3 (1983).
- [69] Xie, Edwards Allen, Noah Fahlgren, Adam Calamar, Scott A. Givan, James C. Carrington, Expression of Arabidopsis MIRNA Genes, *American Society of Plant Biologists*, **138**, p. 2145 (2005).
- [70] Xuejing Zheng, Makarand S. Pimplapure, Günter Weickert, Joachim Loos, Study the Porosity Effects of Ziegler Natta Catalyst on Polymerization System, *European polymer journal*, **68**, p. 680 (2006).
- [71] Xie T.T., McAuley K.B., Hsu J.C.C., Bacon D.W., Gas Phase Ethylene Modeling, *Ind. Eng. Chem. Res.*, **33**, p. 449 (1994).
- [72] Zabrodsky S.S., "Hydrodynamics and Heat Transfer in Fluidized Beds". MIT Press, Cambridge, MA, U.S.A (1966).
- [73] Ye Y., "Interior Point Algorithms for Quadratic Programming", Paper Series No. 89-29, Dept. of Management Sciences, University of Iowa, Iowa City, (1988).
- [74] Victor M. Zavala, Antonio Flores-Tlacuahuac and Eduardo Vivaldo-Lima, Dynamic optimization of a Semi-Batch Reactor for Polyurethane Production, *Chemical Engineering Science*, **60**, p. 3061 (2005).
- [75] Zeybek Z., Yüce S., Hapolu H., Alpaz M., Adaptive Heuristic Temperature Control of a Batch Polymerisation Reactor, *Chemical Engineering and Processing*, **43**(7), p. 911 (2004).
- [76] Vieira R.A.M., Embiruçu M., Sayer C., Pinto J.C., Lima E.L., Control Strategies for Complex Chemical Processes. Applications in Polymerization Processes, *Computers & Chemical Engineering*, **27**(8-9), p. 1307 (2003).
- [77] Zhihua Xiong, Jie Zhang, Modelling and Optimal Control of Fed-Batch Processes Using a Novel Control Affine Feed Forward Neural Network, *Neurocomputing*, **61**, p. 317 (2004).
- [78] Yuan Tian, Jie Zhang, Julian Morris, Optimal Control of a Batch Emulsion Copolymerisation Reactor Based on Recurrent Neural Network Models, *Chemical Engineering and Processing*, **41**(6), p. 531 (2002).
- [79] Yaohui [Reference to Lu], Yaman, Quasi-Min-Max MPC Algorithms for LPV Systems, *Automatica*, **36**(4), p. 527 (2000).